



25^{ème} Forum des microscopies à sondes locales

AFM-IR, spectroscopie et imagerie infrarouge à l'échelle nanométrique : *Principe et applications*

Pr. Alexandre Dazzi, Université Paris-Saclay, France

Table of content

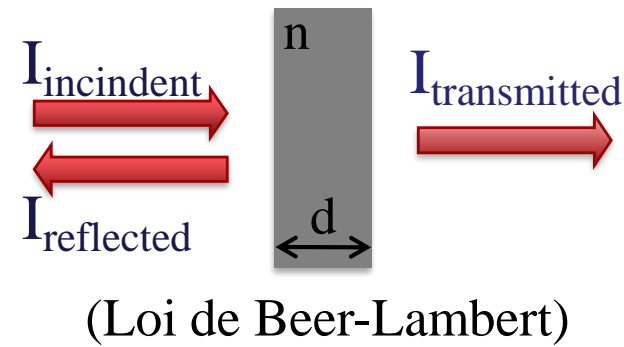
1. Conventional IR spectroscopy and imaging
2. AFM-IR technique: concept and theory
3. Applications examples
4. Evolution of the technique in scientific and industrial field.
5. Comparison with competitors

1. Conventional IR spectroscopy and imaging

Spectroscopy principle:

Transmittance

$$T = \frac{I_t}{I_{inc}}$$

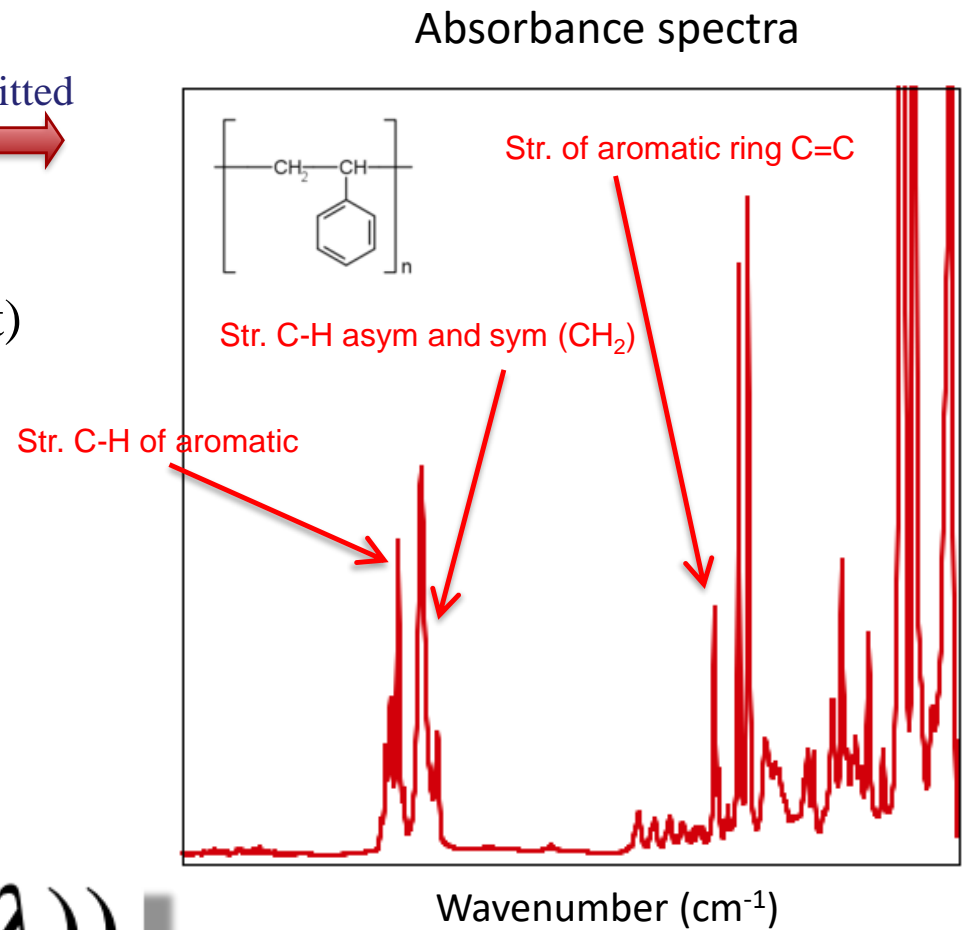


(Loi de Beer-Lambert)

Absorbance

$$A = \log_{10} \frac{I_{inc}}{I_t} = \frac{1}{\ln 10} \frac{4\rho}{n_i d}$$

$$\text{Absorbance} \propto \frac{\text{Im}(n(\lambda))}{\lambda}$$



1. Conventional IR spectroscopy and imaging

Coupling spectrometer and microscope



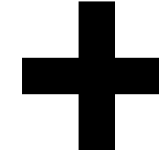
Mode	Theoretical resolution	Experimental resolution
Transmission	2λ	~10-30 μm
ATR	0.5λ	~3-10 μm

2. AFM-IR theory and concept

AFM (Atomic Force Microscope)



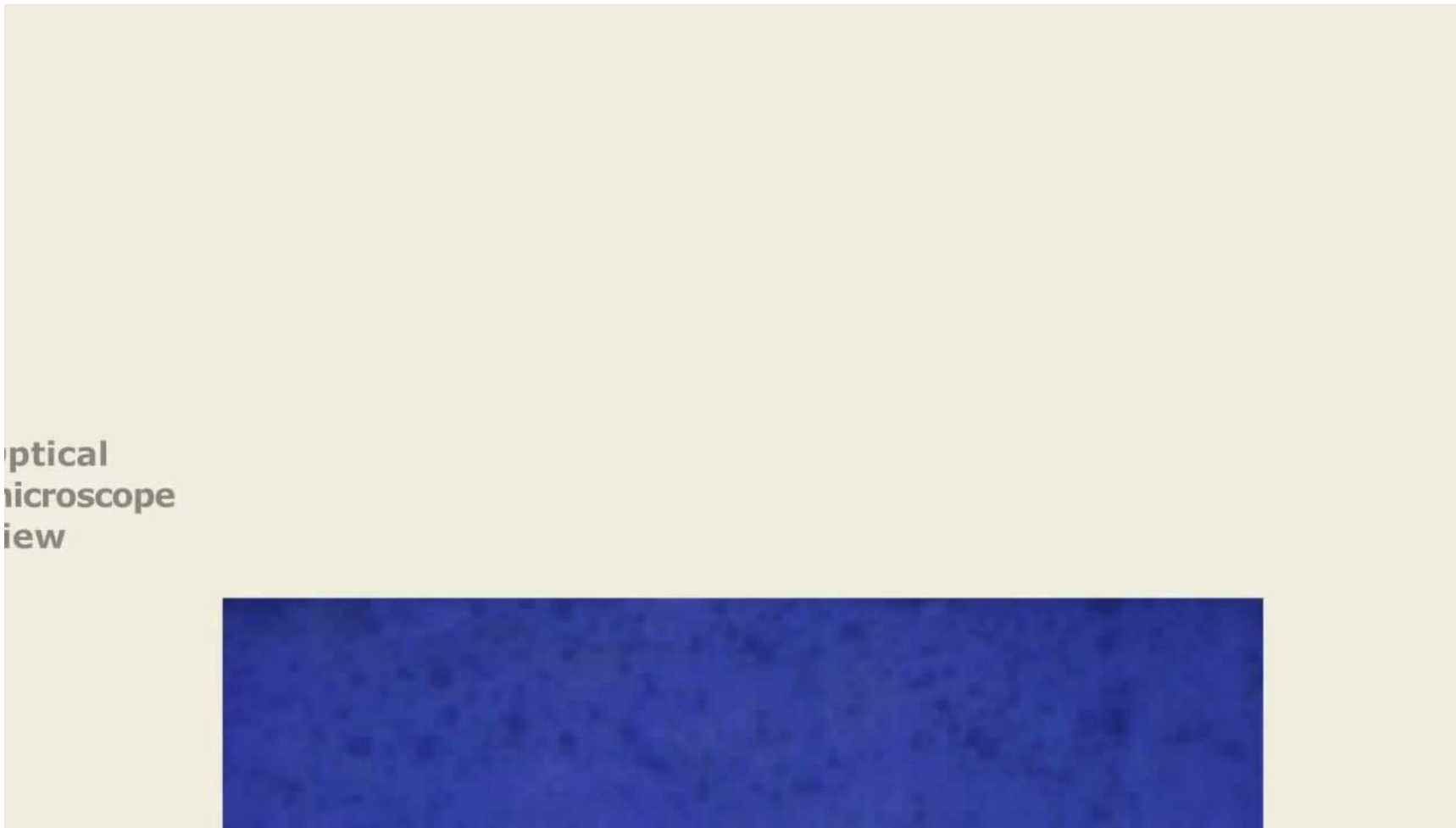
InfraRed laser



AFM-IR

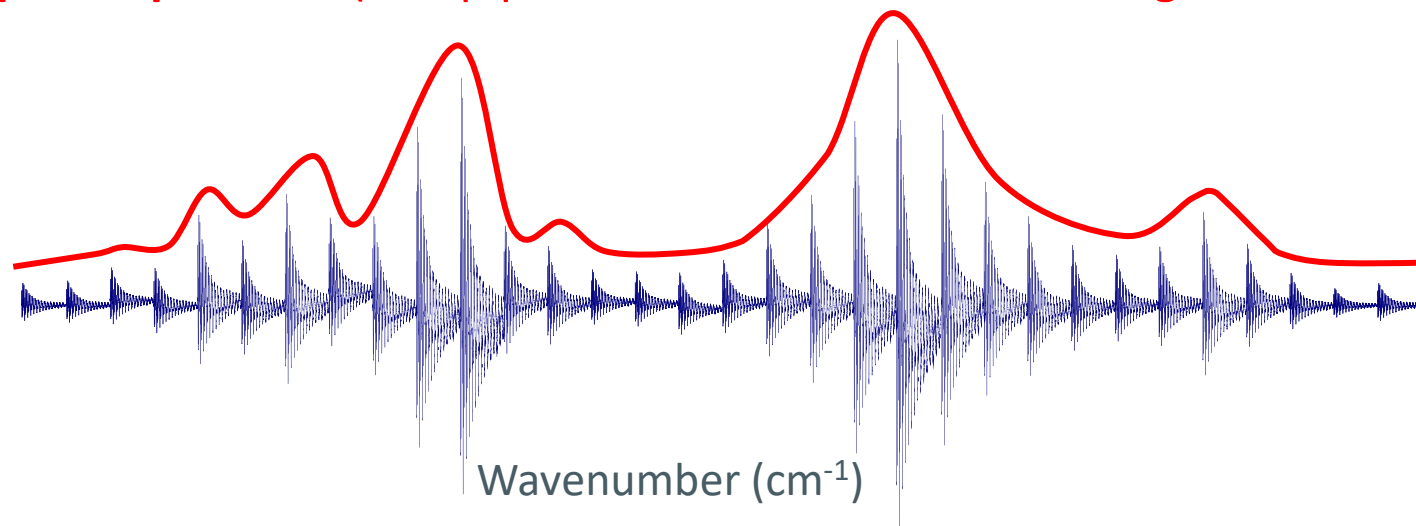
Infrared spectroscopy and imaging at nanometer scale

AFM-IR technique principle

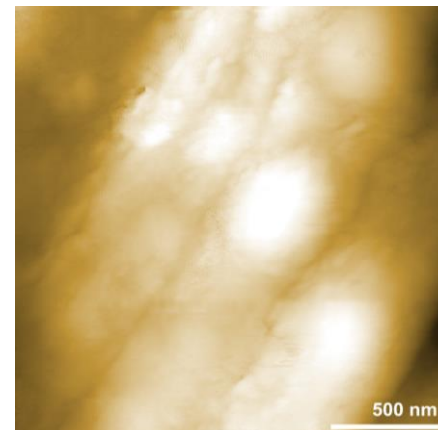


2. AFM-IR theory and concept

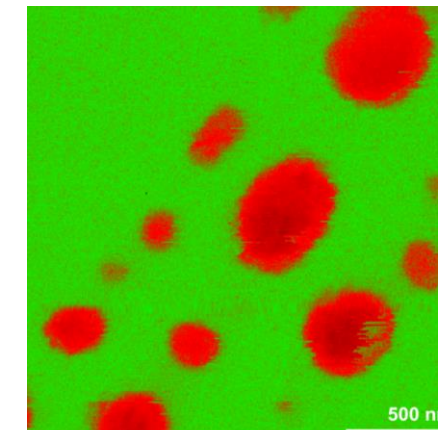
- **Absorption Spectrum** (fix tip position and scan the wavelength of the laser)



- **Chemical mapping** (fix the laser wavelength and scan the surface with the tip)



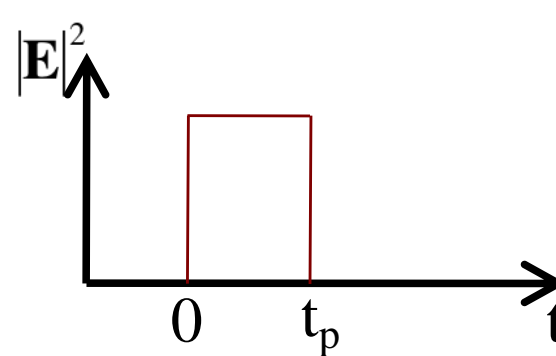
topography



Chemical mapping ($\lambda=5,76\mu\text{m}$)

2. AFM-IR theory and concept

Laser illumination



a sphere radius
 V volume
 n refractive index

Absorbed power

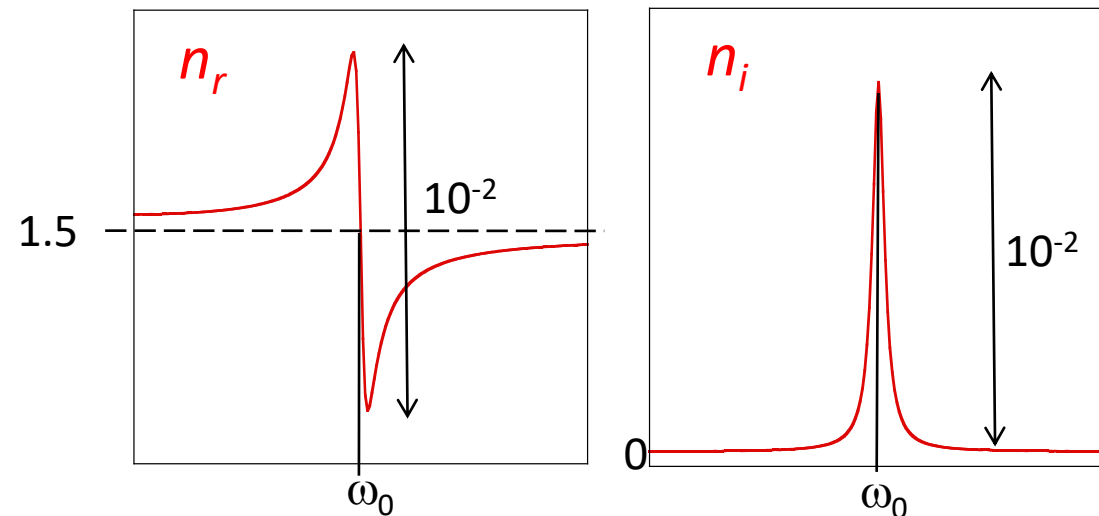
$$P_{abs} = \int_V \frac{\omega \epsilon_0}{2} \text{Im}[n^2(\lambda)] |E_{loc}|^2 dV$$

si $a \ll \perp$

$$P_{abs} = \frac{2\pi}{\lambda} c \epsilon_0 \frac{9 \text{Im}(n) \text{Re}(n)}{\left(\text{Re}(n)^2 + 2 \right)^2} |E_{inc}|^2 V$$

2. AFM-IR theory and concept

Organic matter
 $n_i \ll n_r$



$$P_{abs} = \frac{2\pi}{\lambda} c \epsilon_0 \frac{9 \operatorname{Im}(n) \operatorname{Re}(n)}{\left(\operatorname{Re}(n)^2 + 2\right)^2} |E_{inc}|^2 V$$

$$P_{abs} \propto \frac{\operatorname{Im}(n)}{\lambda} \propto \text{Absorbance}$$

Heat equation:

$$\rho_{sph} C_{sph} \frac{\partial T}{\partial t} = K_{sph} \Delta T + \frac{P_{abs}(t)}{V}$$

\rangle density, C heat capacity, K thermal conductivity

2. AFM-IR theory and concept

Temperature evolution of the sphere

($a \ll L$)

$$T = \frac{T_{\max}}{t_p} t - \frac{(t-t_p)}{\tau_{relax}}$$

when $0 \leq t \leq t_p$

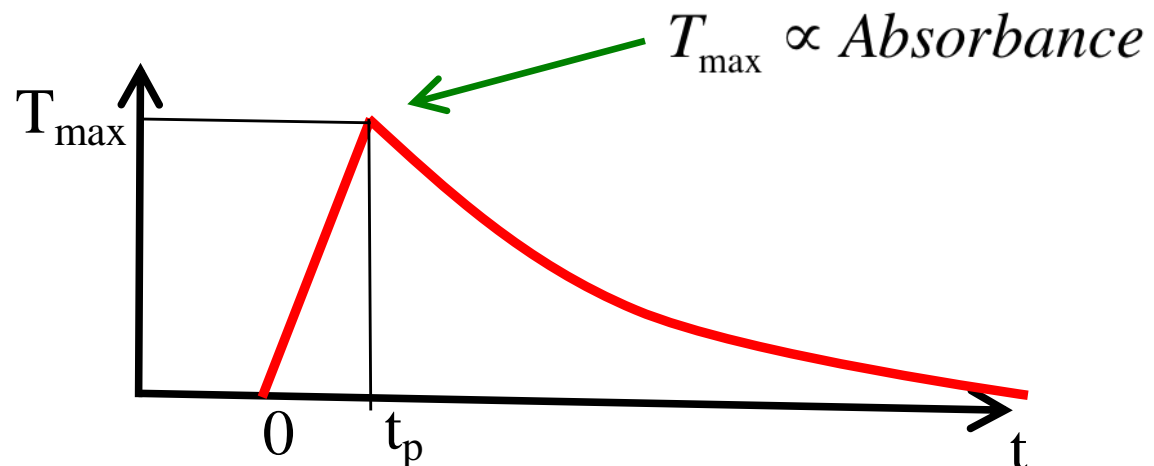
$$T = T_{\max} e^{-\frac{t}{\tau_{relax}}}$$

when $t_p \leq t$

$$T_{\max} = \frac{P_{abs} t_p}{\rho_{sph} C_{sph} V}$$

$$\tau_{relax} = \frac{\rho_{sph} C_{sph}}{3 K_{ext}} a^2$$

Only when $t_p \ll \tau_{relax}$



Localized photothermal infrared spectroscopy using a proximal probe

L. Bozec,^{a)} A. Hammiche, H. M. Pollock,^{b)} and M. Conroy

Department of Physics, Lancaster University, Lancaster LA1 4YB, England

J. M. Chalmers

*V S Consulting, Stokesley, Middlesborough TS9 5NW, United Kingdom
and School of Chemistry, University of Nottingham, University Park, Nottingham, United Kingdom*

N. J. Everall

Science Support Group, ICI plc, Wilton, Middlesborough TS90 8JE, United Kingdom

L. Turin

Department of Physiology, University College London, London WC1E 6BT, United Kingdom

different types of samples (1–6). For example, photoacoustic spectroscopy (PAS) (1–4) involves the detection with a sensitive microphone of the pressure fluctuations in a gas arising from heat produced by the absorption of radiation from a modulated light beam. This technique has the advantage of not requiring optical detection of transmitted or reflected light, and it can be applied to samples which are difficult to examine by conventional spectroscopic methods. Thermal detection methods also have been suggested for the determination of absolute quantum yields by employing calorimetric techniques which are free from the geometrical correction problems of optical methods (5–8). These have also frequently employed microphone detectors (6, 8) or the

application of enzymes (9). Photothermal infrared spectroscopy (PTS), i.e., the use of infrared radiation to heat a sample (i.e., the sample with high thermal absorption coefficient) and then to detect the infrared absorption of the sample (10–12) has been used to study PTS showing absorption bands with a large first

ANALYTICAL

Resolution bigger than a few micrometers !

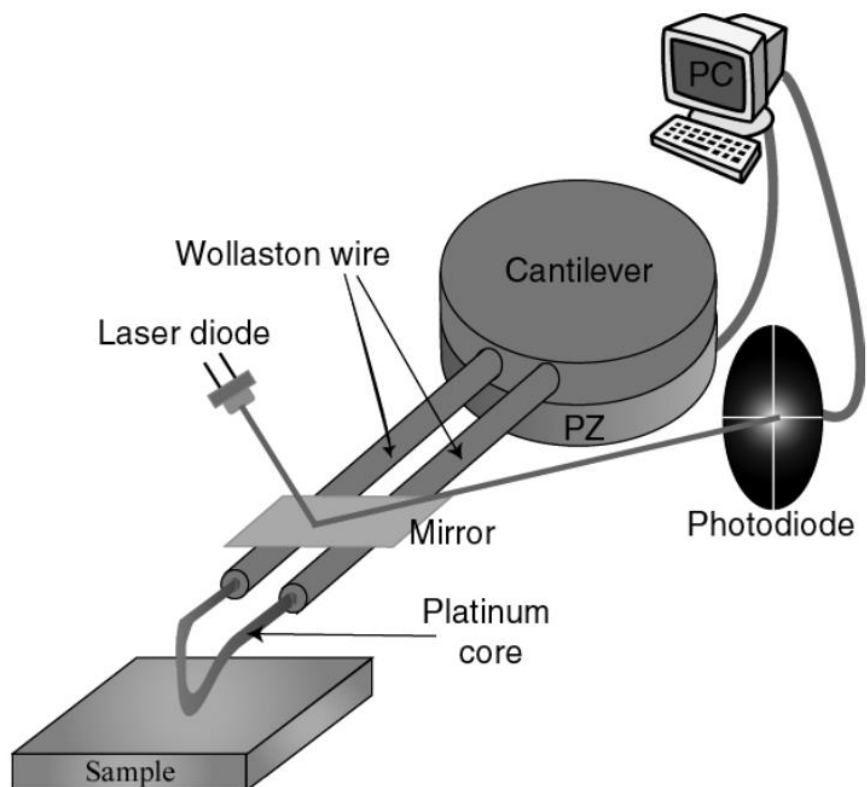


Figure 4: STHM schematic view

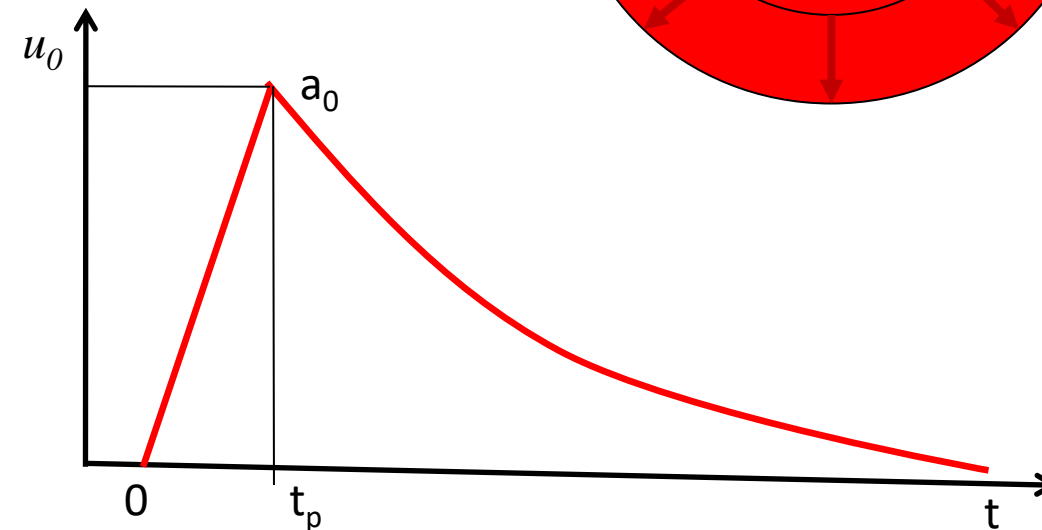
2. AFM-IR theory and concept

Evolution of the sphere deformation

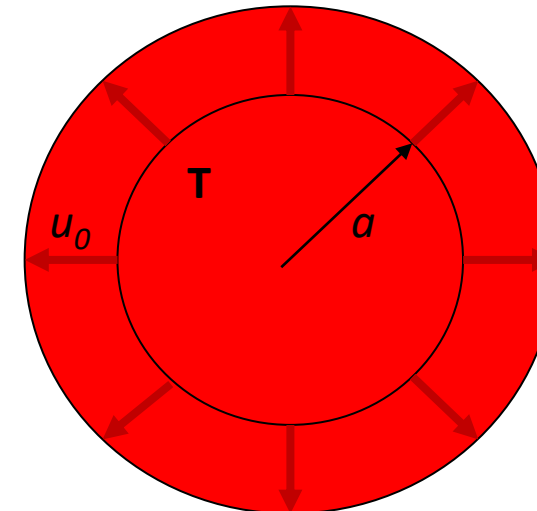
$$(1 - 2\nu)\nabla^2\vec{u} + \nabla(\nabla\vec{u}) = 2(1 + \nu)\alpha_{sph}\nabla T$$

$$\frac{u_0(t)}{a} = \frac{1 + \nu}{1 - \nu} \frac{\alpha_{sph}}{3} T(t)$$

α_{sph} thermal expansion coefficient
 ν Poisson coefficient



$$a_0 = \frac{1 + \nu}{1 - \nu} \frac{a}{3} \alpha_{sph} T_{\max} = \frac{1 + \nu}{1 - \nu} \frac{a \alpha_{sph} P_{abs} t_p}{3 r_{sph} C_{sph} V} \mu \text{Absorbance}$$



ART. XXXIV.—*On the Production and Reproduction of Sound by Light*; by ALEXANDER GRAHAM BELL, Ph.D.

[Read before the American Association for the Advancement of Science, in Boston, August 27, 1880.]

IN bringing before you some discoveries made by Mr. Sumner Tainter and myself, which have resulted in the construction of apparatus for the production and reproduction of sound by means of light, it is necessary to explain the state of knowledge which formed the starting point of our experiments.

I shall first describe that remarkable substance "selenium," and the manipulations devised by previous experimenters; but the final result of our researches has widened the class of substances sensitive to light vibrations, until we can propound the fact of such sensitiveness being a general property of all matter.

We have found this property in gold, silver, platinum, iron, steel, brass, copper, zinc, lead, antimony, german-silver, Jenkins's metal, Babbitt's metal, ivory, celluloid, gutta-percha, hard rubber, soft vulcanized rubber, paper, parchment, wood, mica, and silvered glass; and the only substances from which we have not obtained results, are carbon and thin microscope glass.*

* Later experiments have shown that these are not exceptions.

We find that when a vibratory beam of light falls upon these substances *they emit sounds*, the pitch of which depends upon the frequency of the vibratory change in the light. We find farther, that when we control the form or character of the light, vibrations on selenium (and probably on the other substances), we control the quality of the sound, and obtain all varieties of articulate speech. We can thus, without a conducting wire as in electric telephony, speak from station to station wherever we can project a beam of light. We have not had the opportunity of testing the limit to which this photophonic effect may be extended, but we have spoken to and from points 213 meters apart; and there seems no reason to doubt that the results will be obtained at whatever distance a beam of light can be flashed from one observatory to another. The necessary privacy of our experiments, hitherto, has alone prevented any attempts at determining the extreme distance at which this new method of vocal communication will be available.

The Opto-Acoustic Effect: Revival of an Old Technique for Molecular Spectroscopy

William R. Harshbarger and Melvin B. Robin*

Bell Laboratories, Murray Hill, New Jersey 07974

330

Harshbarger and Robin

Accounts of Chemical Research

Over 90 years ago, described qualitatively treatments which have gone unceasing generations until the present.¹

In his pioneering experiments, he dispersed sunlight onto a prism between the sample tube and a rotating slotted disk. If a solid, liquid, or gas is adsorbed, then the "absorptance" through an attenuator length of tubing connected to the cell, with the other end entering the lamp. The frequency of the pulses at which the light was cho-

The transformation is easy to see: the pulses are degraded in the sample gas express themselves as sound. In summarizing his results, he wrote:

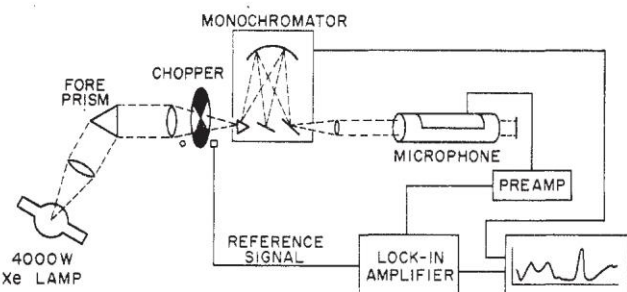


Figure 1. Experimental setup for opto-acoustic spectroscopy.

offers the possibility of observing absorption at the parts per 10^6 level or, for a gas at 1-atm pressure in the cell, the possibility of observing transitions with an oscillator strength of only 10^{-12} or so. This is the feature which first attracted us to the technique, but we have not yet realized the anticipated sensitivity.

Under what conditions does absorption lead to a signal at the microphone? In general, following electronic excitation, a molecule has three channels open to it: (i) it may luminesce, leaving little or no heat in the molecule; (ii) it may undergo a chemical reaction,

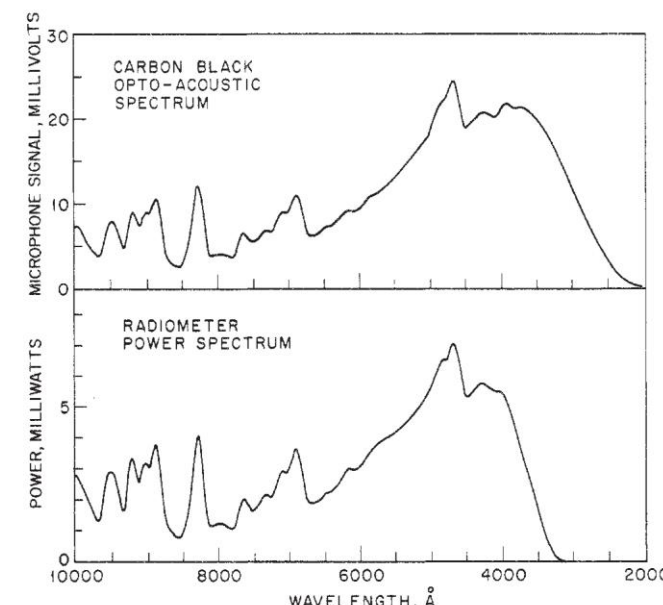


Figure 2. Comparison of the carbon black opto-acoustic spectrum with that of a calibrated radiometer.

2. AFM-IR theory and concept

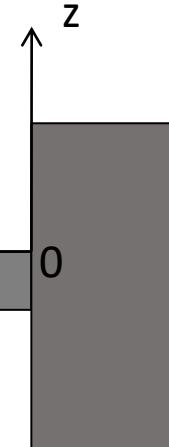
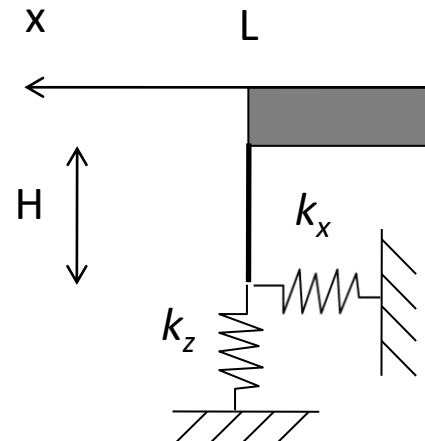
Differential equation of cantilever motion :

$$EI \frac{\partial^4 z}{\partial x^4} + rA \frac{\partial^2 z}{\partial t^2} + k \frac{\partial z}{\partial t} = 0$$

E Young modulus, I inertia moment, ρ density, A section, κ damping

with k_c cantilever spring constant:

$$k_c = \frac{3EI}{L^3}$$



L length, H tip height,
 k_x lateral spring constant, k_z normal spring constant

$k_z \gg k_c$ **NO indentation**

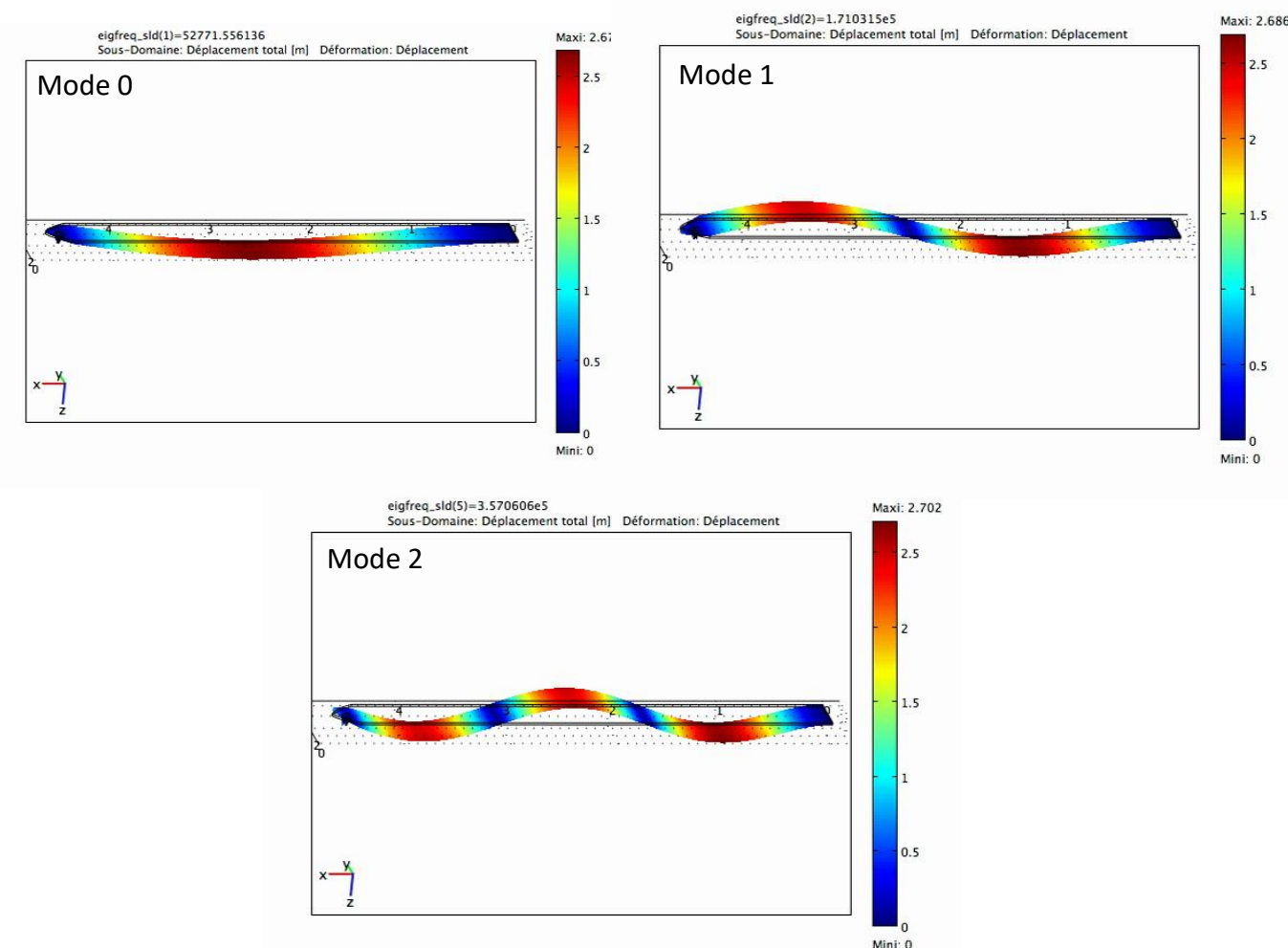
2. AFM-IR theory and concept

$$-1 + \cos X \cosh X - UX(\sin X \cosh X - \cos X \sinh X) = 0$$

with $U = \frac{k_c L^2}{3k_x H^2}, X = bL$

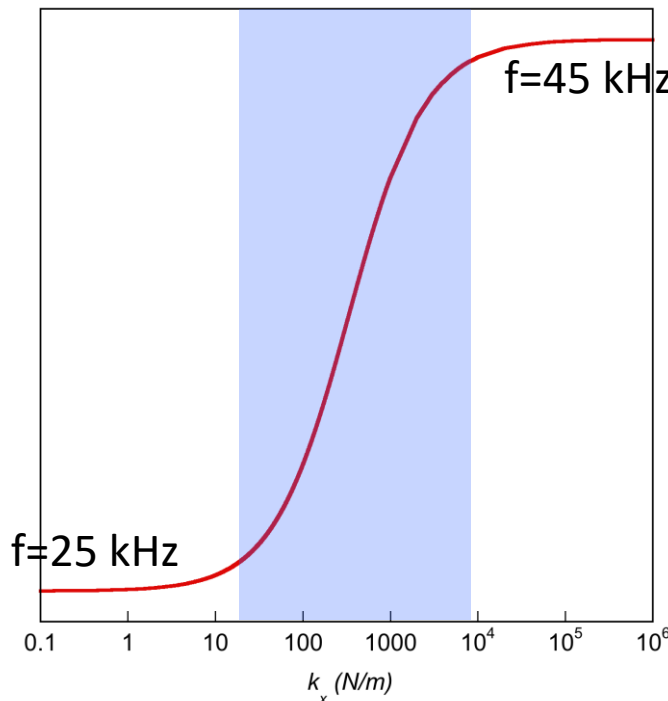
Cantilever Si contact

k_x	0 (pure sliding)	∞ (pinned)
Mode	$X_n = \beta_n L$	$X_n = \beta_n L$
0	3.92662	4.73004
1	7.06858	7.8532
2	10.3518	14.1372



2. AFM-IR theory and concept

Mechanical sensitivity of contact resonance modes



$$f_n = \frac{1}{2\rho} \sqrt{\frac{k_c}{3\pi AL}} \left(\frac{(X_n^p - X_n^f)}{\zeta(1 + \frac{k_c L^2}{3k_x H^2} \frac{(a_n X_n^p - X_n^f)}{\theta})} \right)^{\frac{1}{2}}$$

X_n^p pinned,
 X_n^f pure sliding,
 a_n modal constant

Mode number n	a_n	X_n^p	X_n^f
0	2.09	4.730040	3.92662
1	2.2524	7.853200	7.06858
2	2.3005	10.99560	10.2102
3	2.3276	14.1372	13.3518

2. AFM-IR theory and concept

Differential equation of cantilever motion with external force :

$$EI \frac{\partial^4 z}{\partial x^4} + rA \frac{\partial^2 z}{\partial t^2} + k z = S(x,t)$$

with $S(x,t)$ external excitation

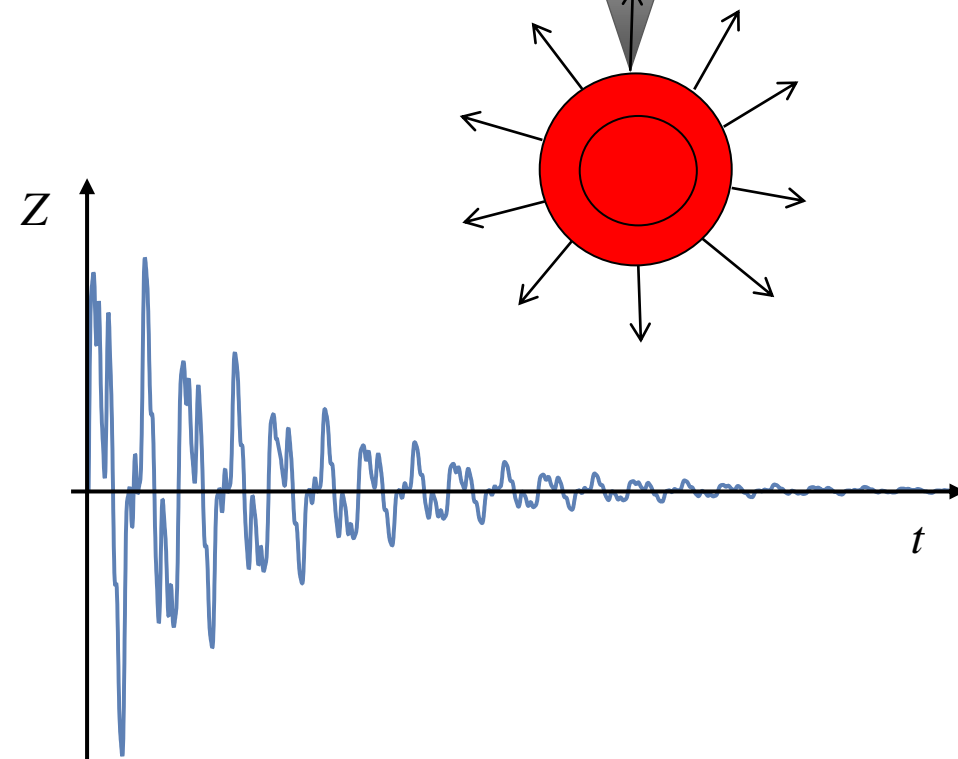
Induced force by the sphere expansion gives :

$$S(x,t) = \delta(x - L + \Delta x) F(t) = B \delta(x - L + \Delta x) T_{sph}(t)$$

Equation solution becomes :

$$z(t) = \sum_n \frac{Kk_z D \delta_x}{\rho S L} \left(\frac{\partial g_n}{\partial x} \Big|_{x=L} \right)^2 \frac{\left(\frac{t_p}{2} + \tau_{relax} \right)}{\omega_n} \sin(\omega_n t) e^{-\frac{\Gamma}{2}t} a_0$$

$$Z(t) \propto a_0 \propto \text{Absorbance}$$



2. AFM-IR theory and concept

Fourier transform of $Z(t)$ signal

$$\tilde{Q}(W) = \sum_n \tilde{Q}_n(W) = \sum_n D |C| \frac{\partial g_n(x)}{\partial x} \Big|_{x=L} \frac{|\tilde{T}_{sph}(W)|}{\sqrt{(W_n^2 - W^2)^2 + G^2 W^2}}$$

Mode amplitude

$$\tilde{Q}_n(W_n) = H_m H_{AFM} H_{opt} H_{th} \frac{\text{Im}(n(\lambda))}{\lambda}$$

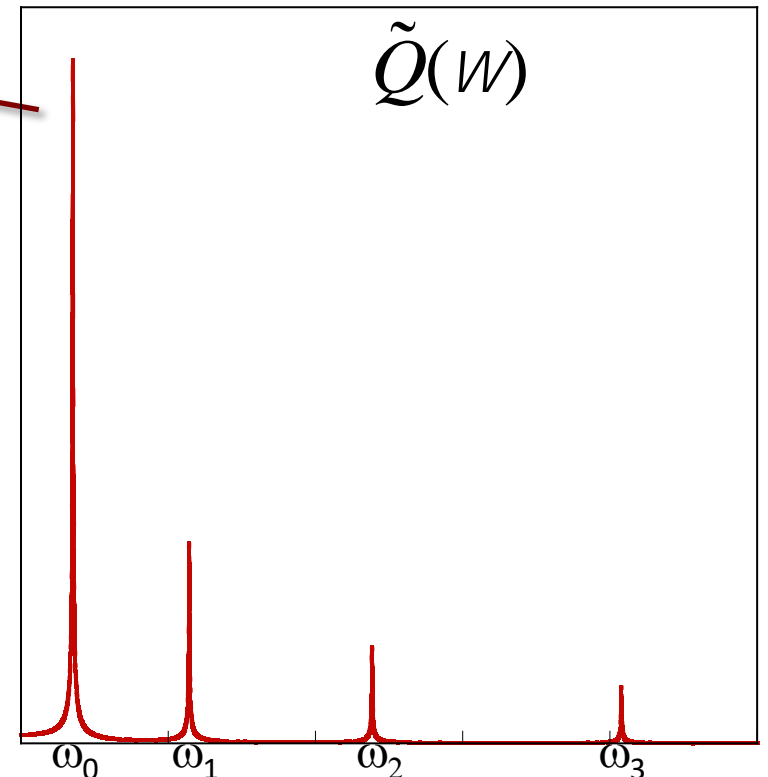
$$H_m = k_z \partial_{sph} a$$

$$H_{AFM} = \frac{1}{G W_n} [\cos(\alpha) dx + \sin(\alpha) H] \frac{D}{m} \frac{\partial g_n(x)}{\partial x} \Big|_{x=L}$$

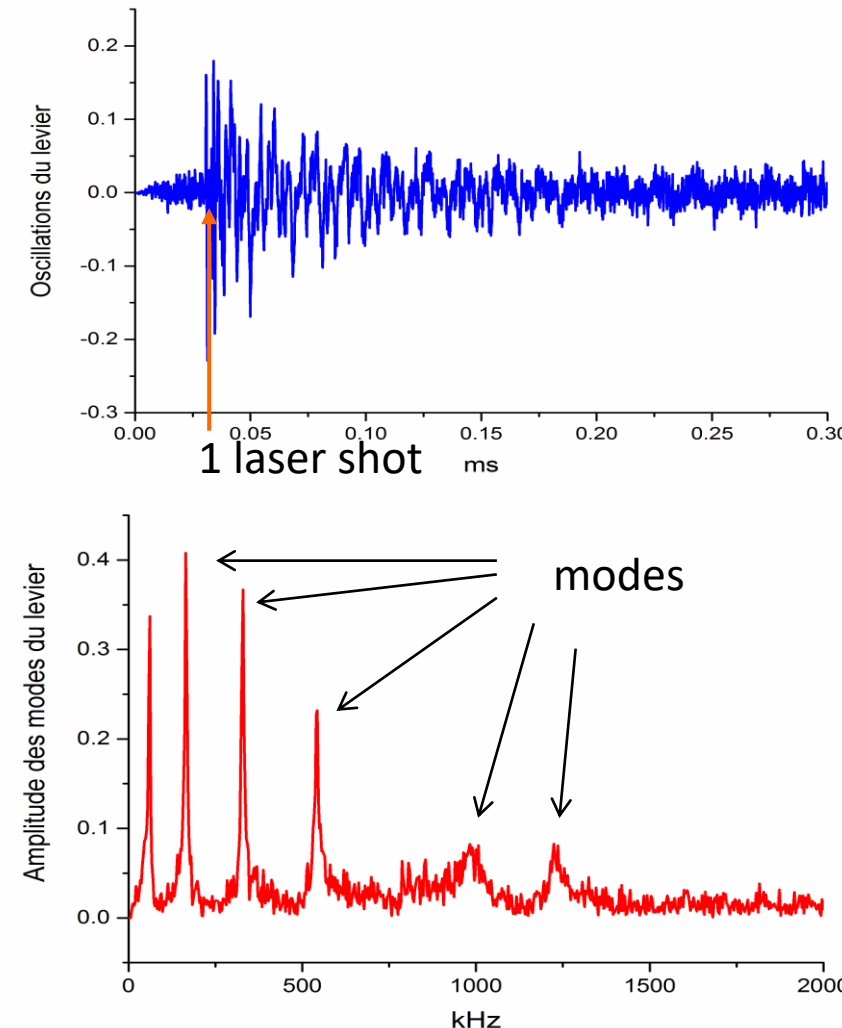
$$H_{opt} = \frac{\text{Re}(n)}{(\text{Re}(n)^2 + 2)^2} c \epsilon_0 |E_{inc}|^2$$

$$H_{th} = \frac{6\rho}{r_{sph} C_{sph}} t_p \frac{\partial t_p}{2} + t_{relax} \frac{\partial}{\partial}$$

$$\tilde{Q}_n(W_n) \propto \frac{\text{Im}(\lambda)}{\lambda} \propto Absorbance$$



2. AFM-IR theory and concept



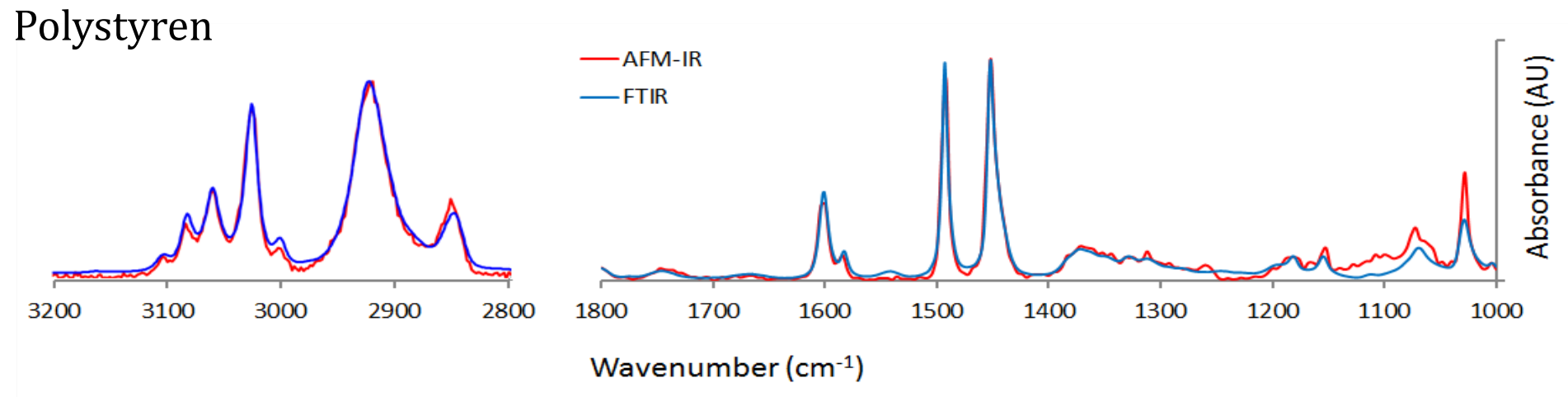
Classical AFM-IR (old version)

2. AFM-IR theory and concept

Classical AFM-IR

Demonstration that photothermal measurement give a direct estimation of imaginary part of the refractive index.

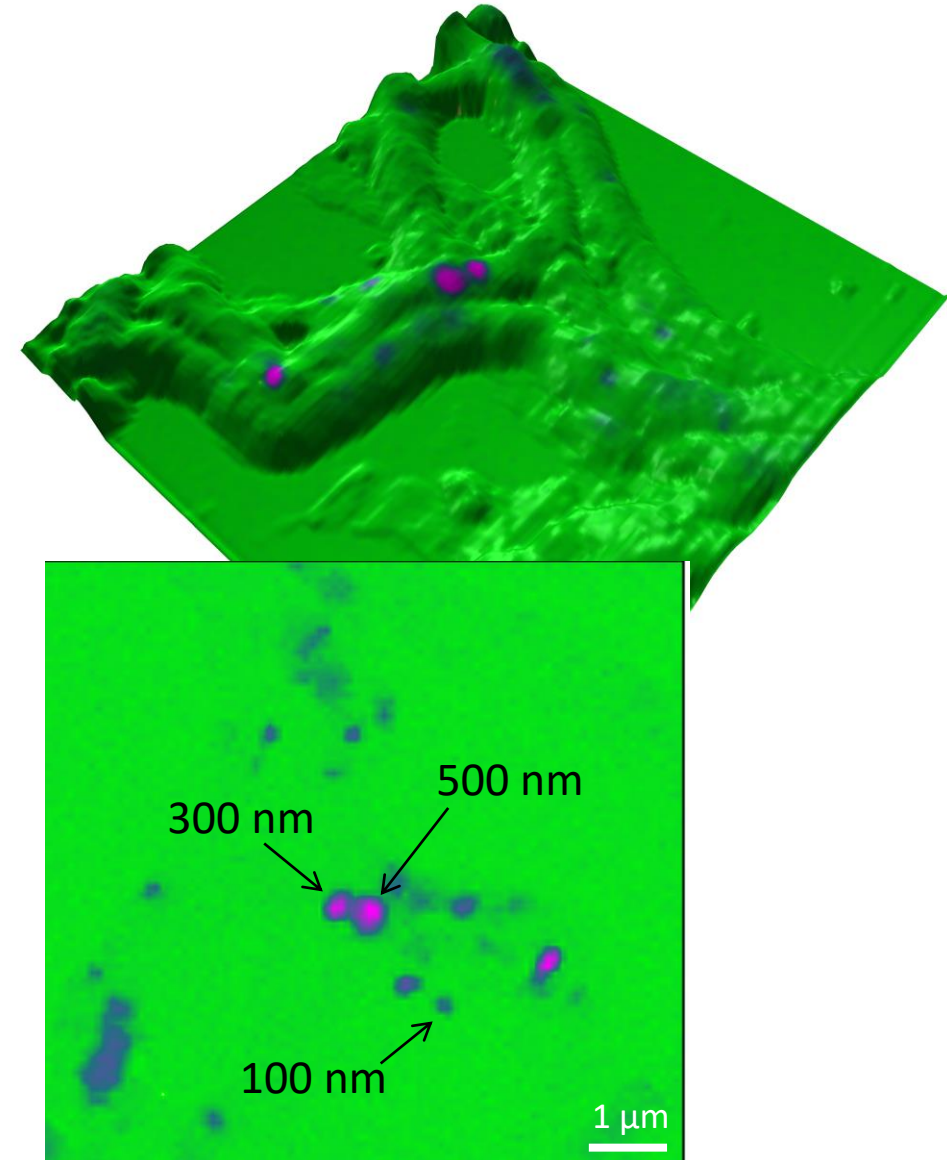
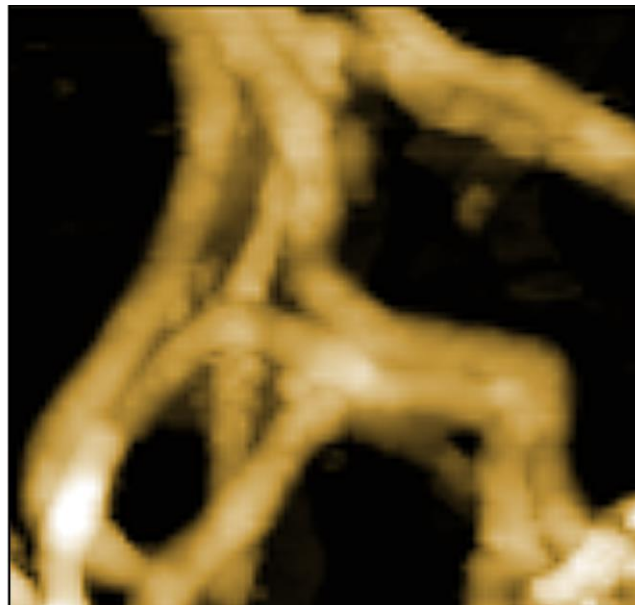
→ AFM-IR Spectrum similar to those obtained by FTIR



2. AFM-IR theory and concept

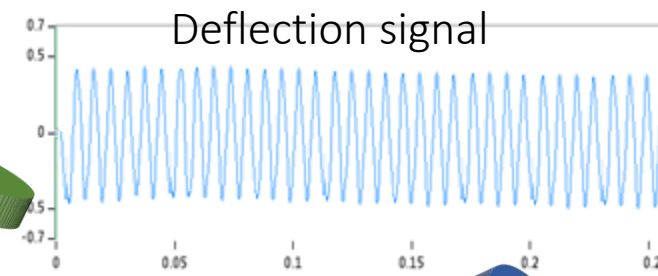
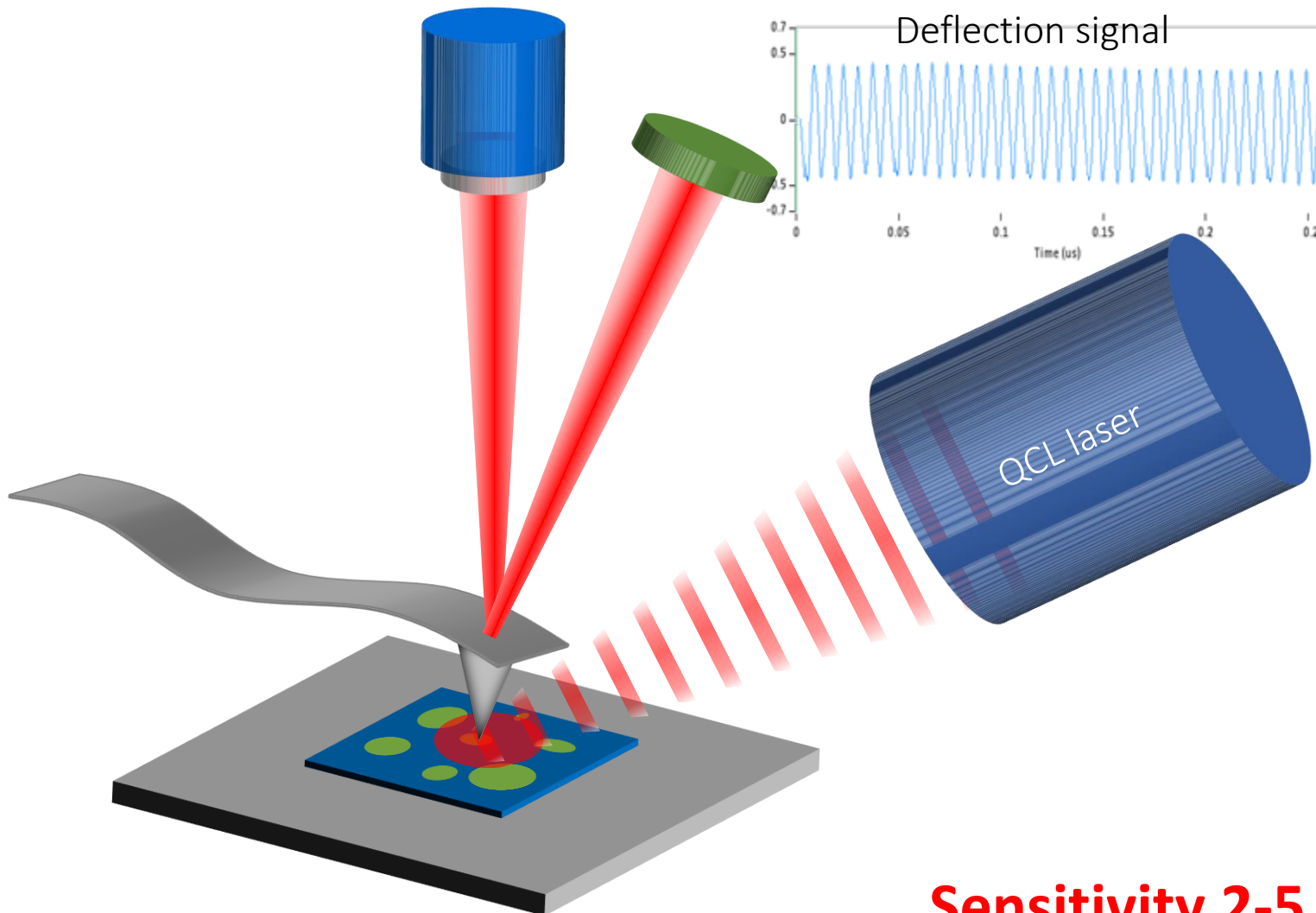
Classical AFM-IR

Detection of lipid vesicles in *Streptomyces bacteria* (1740 cm^{-1})



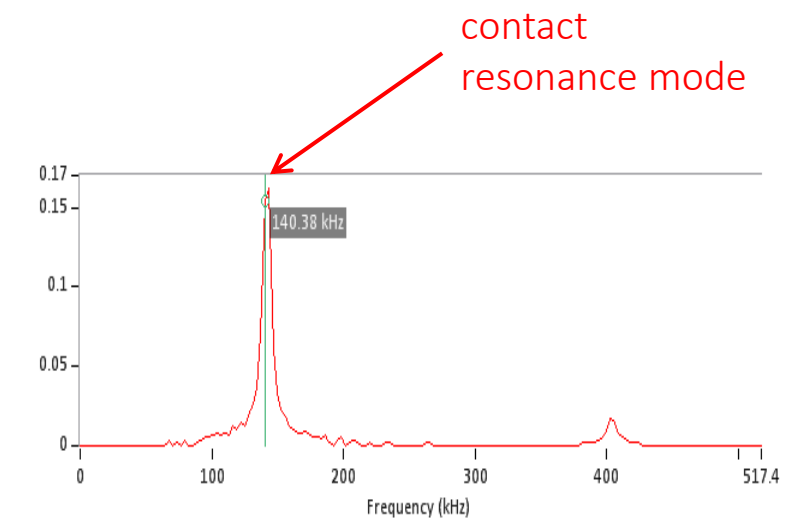
2. AFM-IR theory and concept

AFM-IR imaging mode : contact resonance mode



QCL laser (Quantum Cascade Laser)

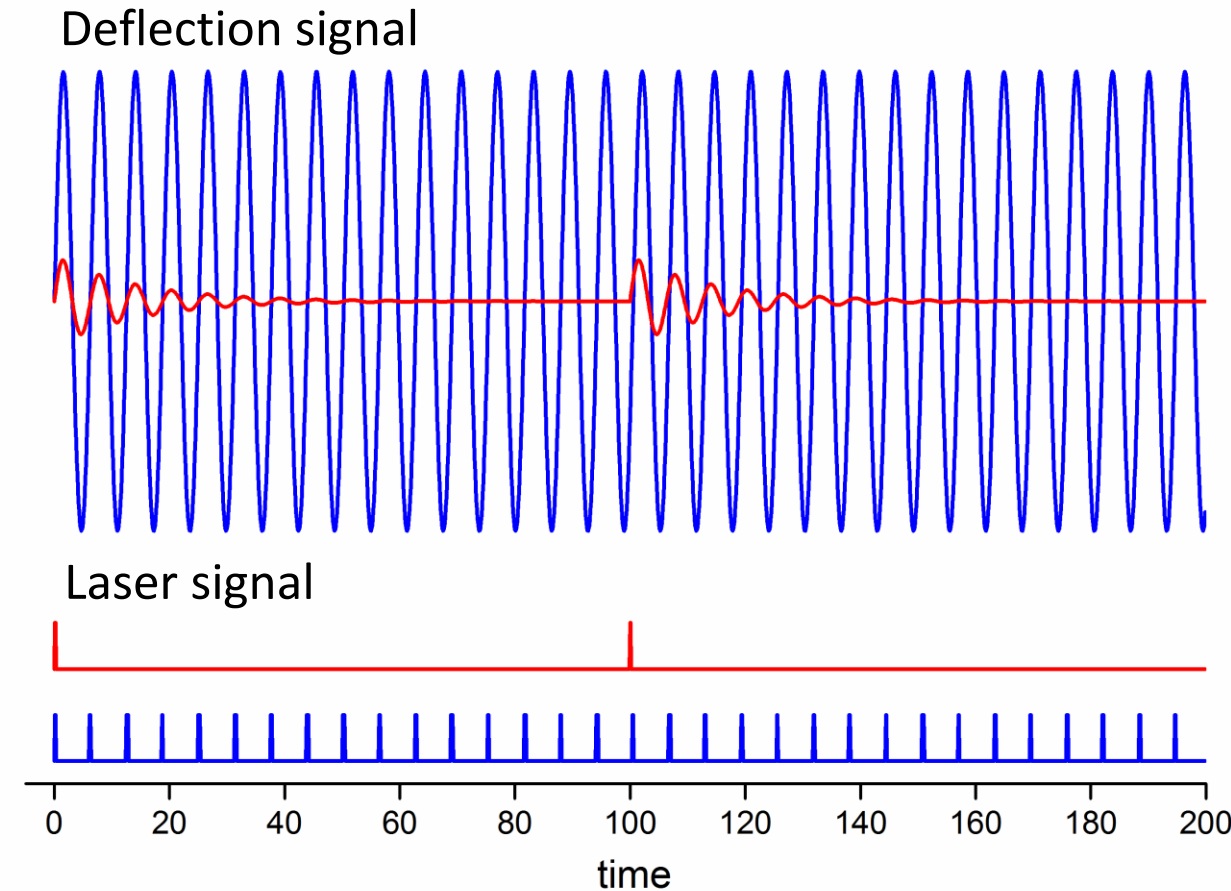
tunable in wavenumber ($1900\text{-}900\text{ cm}^{-1}$)
tunable repetition rate (0-3000 kHz)



Sensitivity 2-5 nm

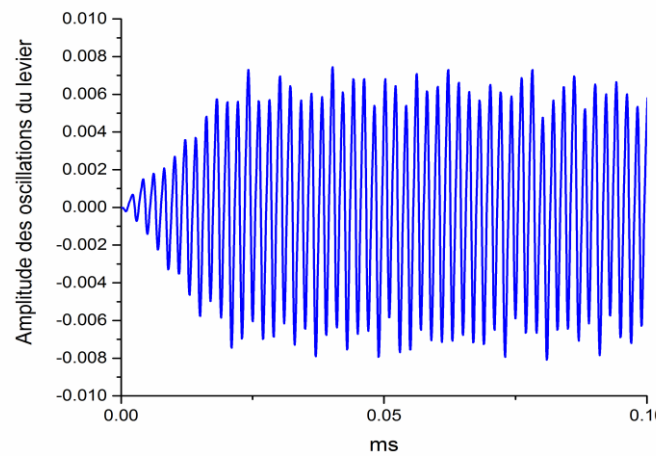
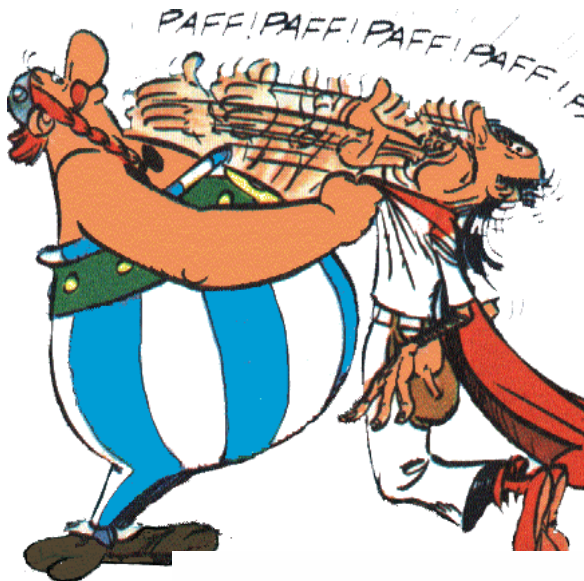
2. AFM-IR theory and concept

AFM-IR imaging mode : contact resonance mode

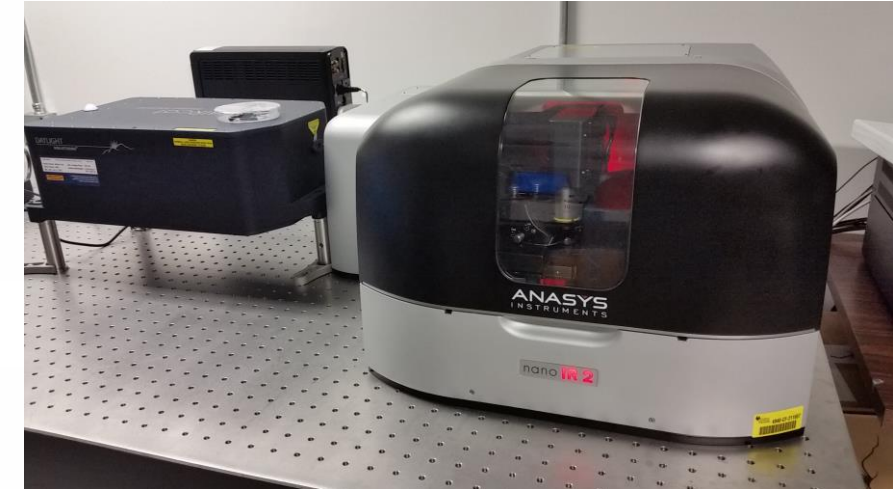
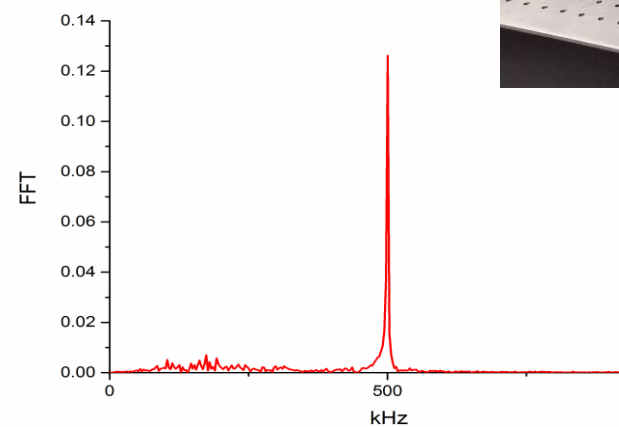
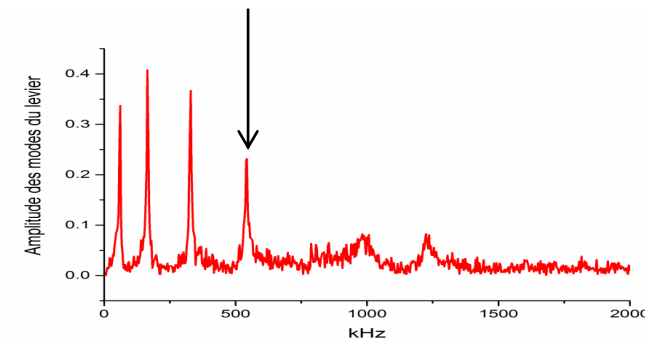


2. AFM-IR theory and concept

Enhanced resonance leads to have a better sensitivity and then better resolution



Laser repetition rate



2. AFM-IR theory and concept

Deflection for 1 pulse (OPO)

$$Z(t) = \sum_n \frac{Kk_z D \delta_x}{\rho S L} \left(\frac{\partial g_n}{\partial x} \Big|_{x=L} \right)^2 \frac{\left(\frac{t_p}{2} + \tau_{relax} \right)}{\omega_n} \sin(\omega_n t) e^{-\frac{\Gamma}{2}t} a_0$$

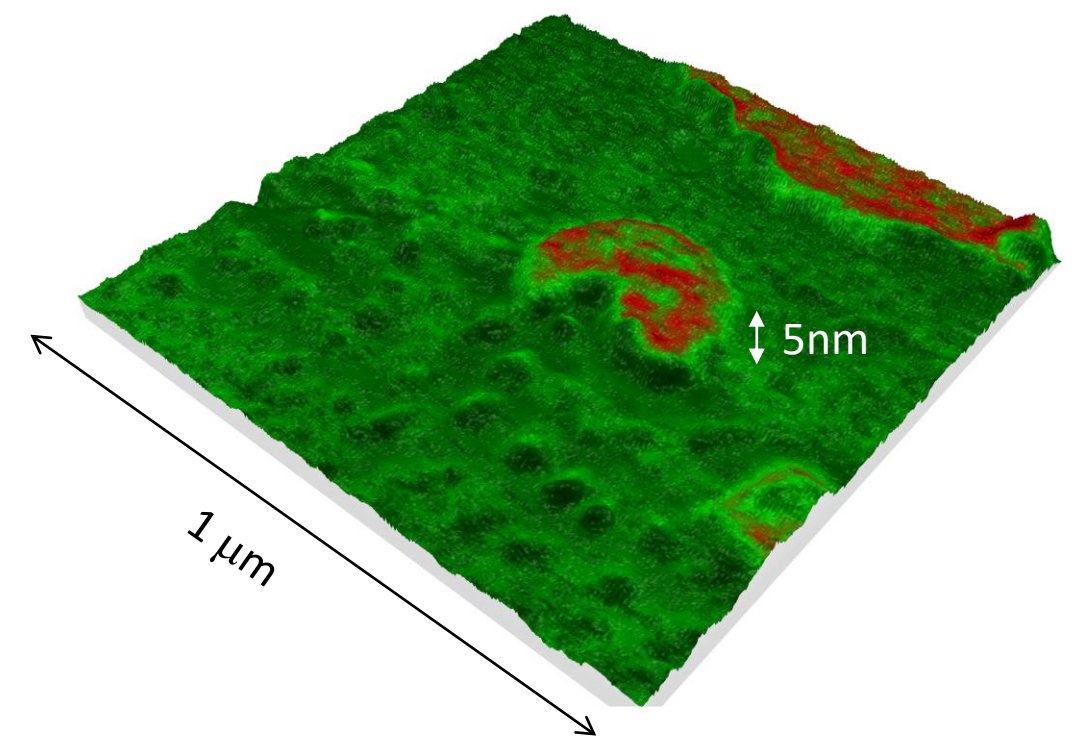
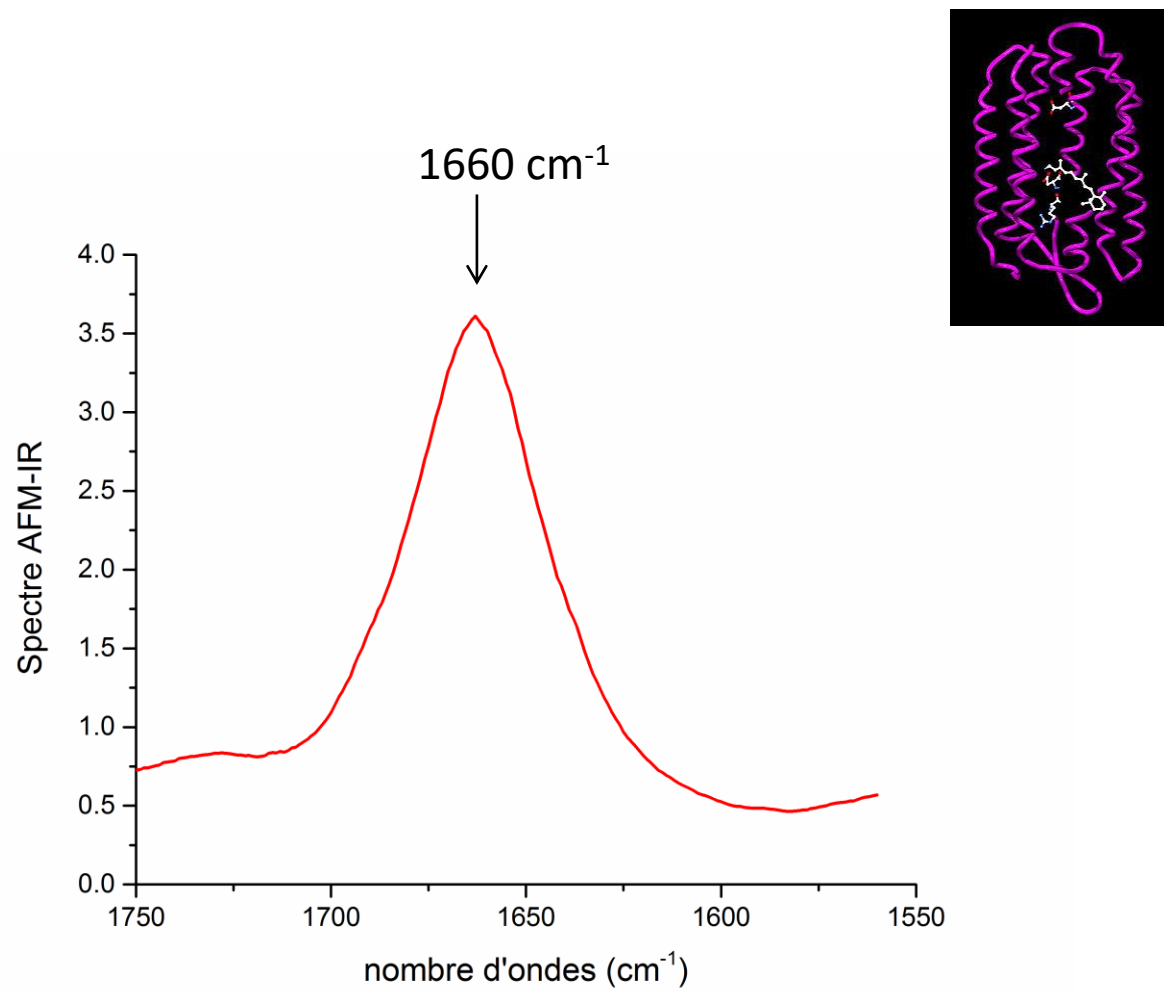
Deflection when repetition rate = contact resonance mode (QCL)

$$Z(t) = \frac{Kk_z D \delta_x}{\rho S L} \left(\frac{\partial g_n}{\partial x} \Big|_{x=L} \right)^2 \frac{\left(\frac{t_p}{2} + \tau_{relax} \right)}{\omega_n} \frac{Q_n}{\pi} \sin(\omega_n t) a_0$$

Amplitude(Z) μ thermal expansion(a_0) μ absorbance

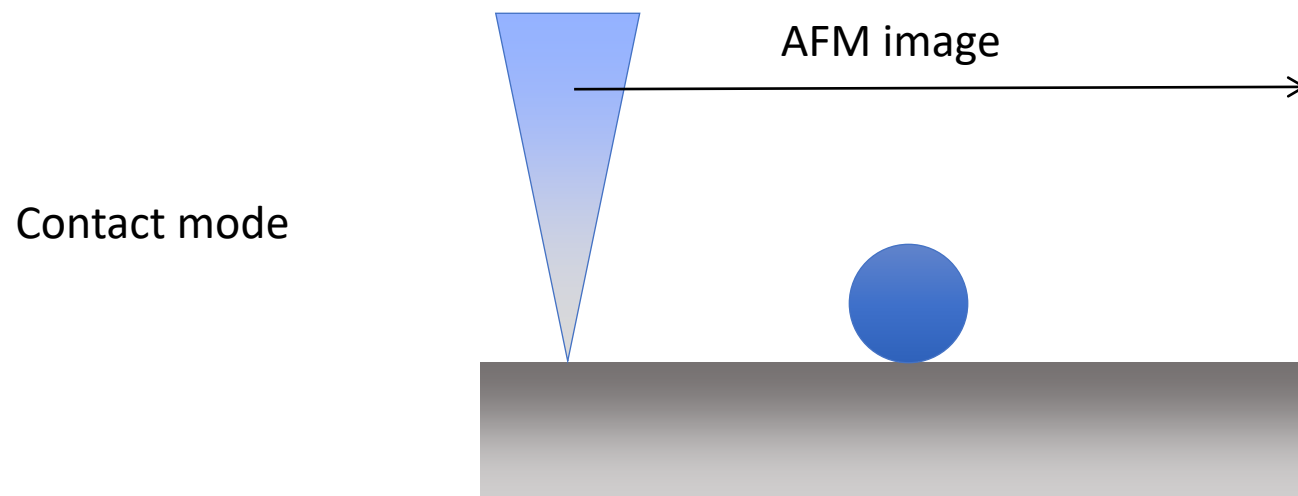
2. AFM-IR theory and concept

Bacteriorhodopsin detection inside a purple membrane

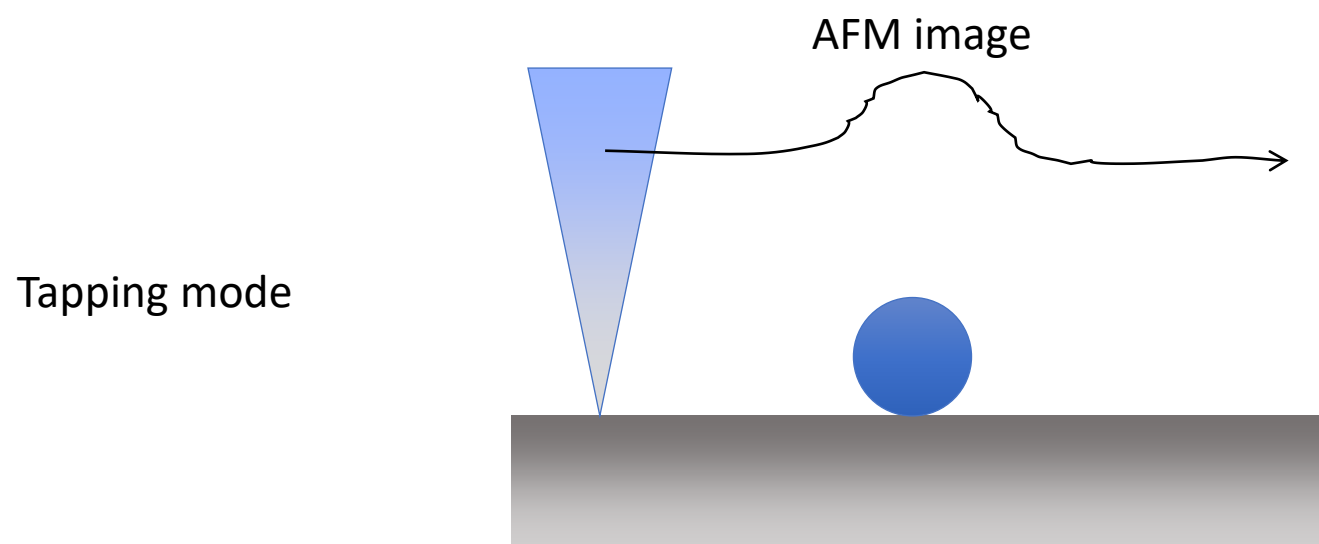


2. AFM-IR theory and concept

AFM-IR imaging mode : tapping AFM-IR



Contact mode



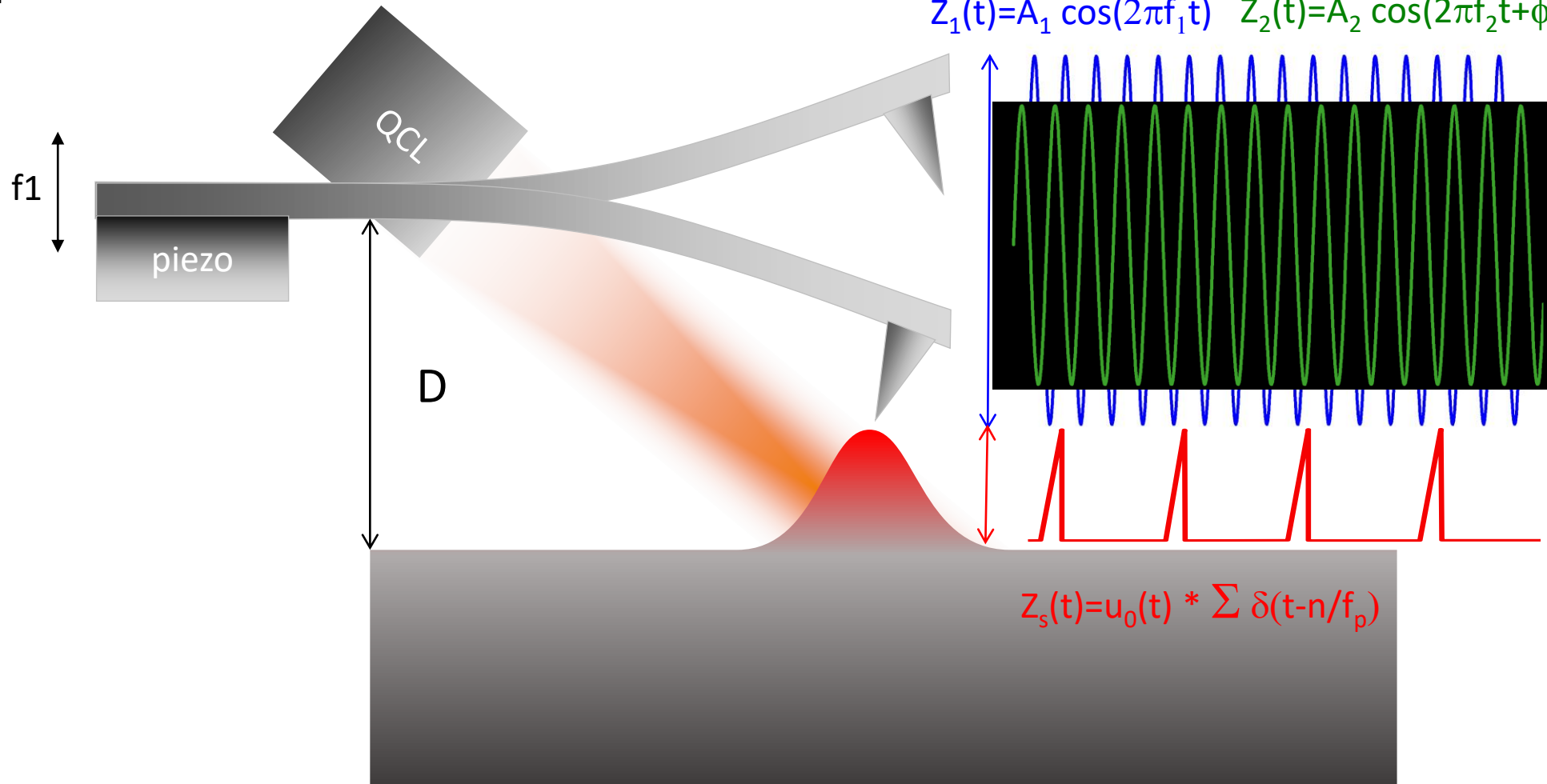
Tapping mode

2. AFM-IR theory and concept

Tapping AFM-IR principle

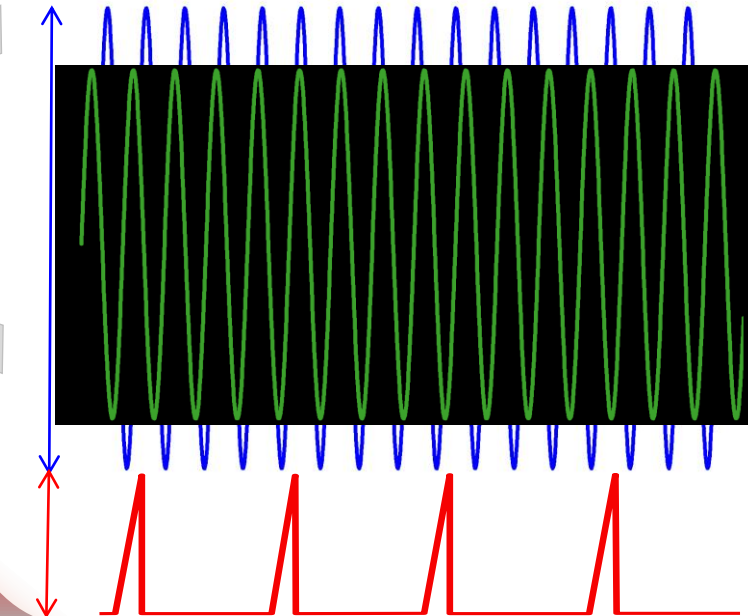
f_1 = drive frequency of tapping mode

f_p = QCL laser frequency



If non linear interaction then: $f_2 = f_1 + f_p$ ou $f_2 = f_1 - f_p$

$$z_1(t) = A_1 \cos(2\pi f_1 t) \quad z_2(t) = A_2 \cos(2\pi f_2 t + \phi_2)$$



$$Z_s(t) = u_0(t) * \sum \delta(t-n/f_p)$$

2. AFM-IR theory and concept

Differential equation of motion for the mode f2 :

$$\ddot{z}_2 + \Gamma \dot{z}_2 + (2\pi f_2)^2 z_2 = \frac{F_{ts}(t)}{m^*}$$

Interaction force between tip and sample surface

$$F_{ts}(t) = K(A_1 \cos(\omega_1 t) - D - u_0(t))^{3/2}$$

$$F_{ts}(t) = k_s (A_1 \cos(\omega_1 t) - u_0(t)) + C_s (A_1 \cos(\omega_1 t) - D - u_0(t))^2 + \dots$$



 \downarrow \downarrow \downarrow \downarrow
 f_1 f_p $2f_1$ $2f_p$

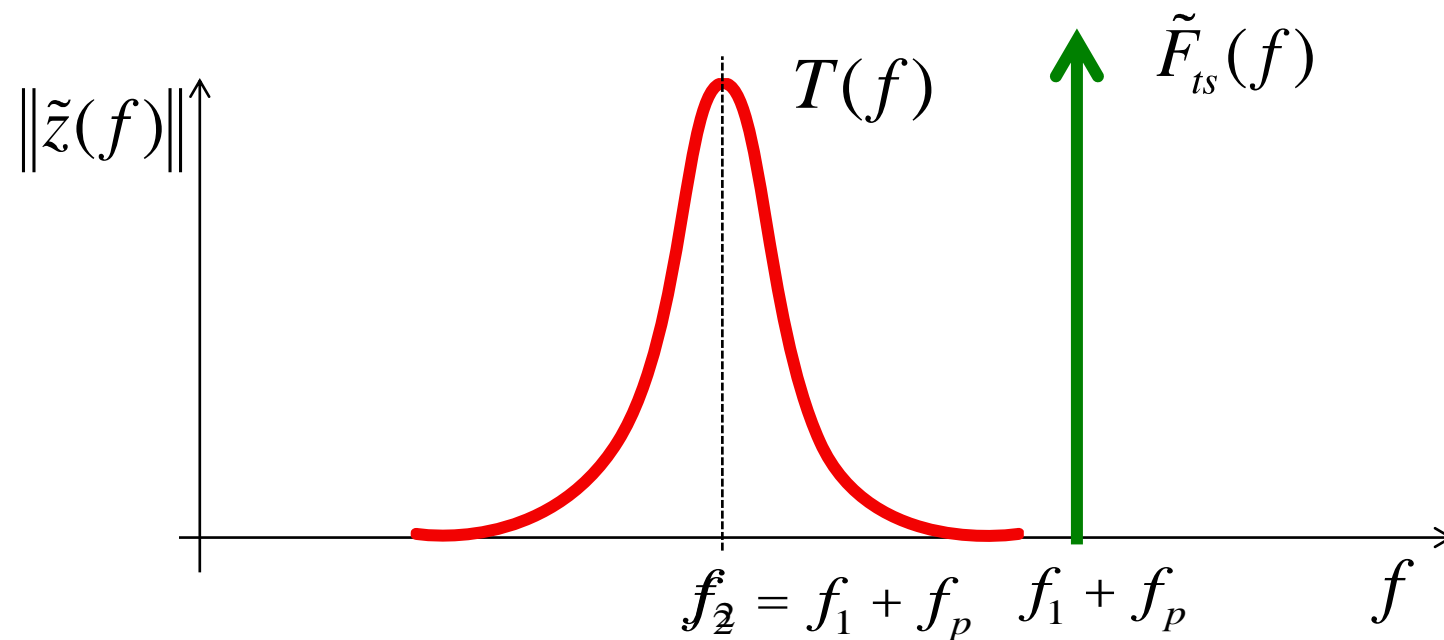
$$F_{ts}(t) = -2 C_s \frac{\ddot{u}_0}{\dot{\tau}} A_1 \cos(2\pi f_1 t) P(t) * \int_m^{\infty} d(t - m/f_1) \frac{\ddot{u}_0}{\dot{\tau}} u_0(t) * \int_n^{\infty} d(t - n/f_p) \frac{\ddot{u}_0}{\dot{\tau}}$$

τ Is the contact time led by f_1

2. AFM-IR theory and concept

$$\ddot{z}_2 + \Gamma \dot{z}_2 + (2\pi f_2)^2 z_2 = \frac{F_{ts}(t)}{m^*} \quad \xrightarrow{\text{Fourier transform}} \quad \tilde{z}_2(f) = \frac{T(f)\tilde{F}_{ts}(f)}{m^*}$$

$$\tilde{F}_{ts}(f) = -(\chi_{ts}\pi A_1 a_0 t_p \tau \omega_1 \omega_p) \delta(\omega - (\omega_1 + \omega_p))$$



2. AFM-IR theory and concept

Mode f₂ ($f_2 = f_1 + f_p$) amplitude give :

$$\|\tilde{z}_2\| = \frac{\chi_{ts} \text{Arc cos}(D / A_1)}{2} t_p \left(\frac{(f_2 - f_1)}{m^* f_2^2} Q_2 (A_1 - D) a_0 \right)$$

non linear elasticity coefficient

Pulse duration

Tapping setpoint

Tapping amplitude

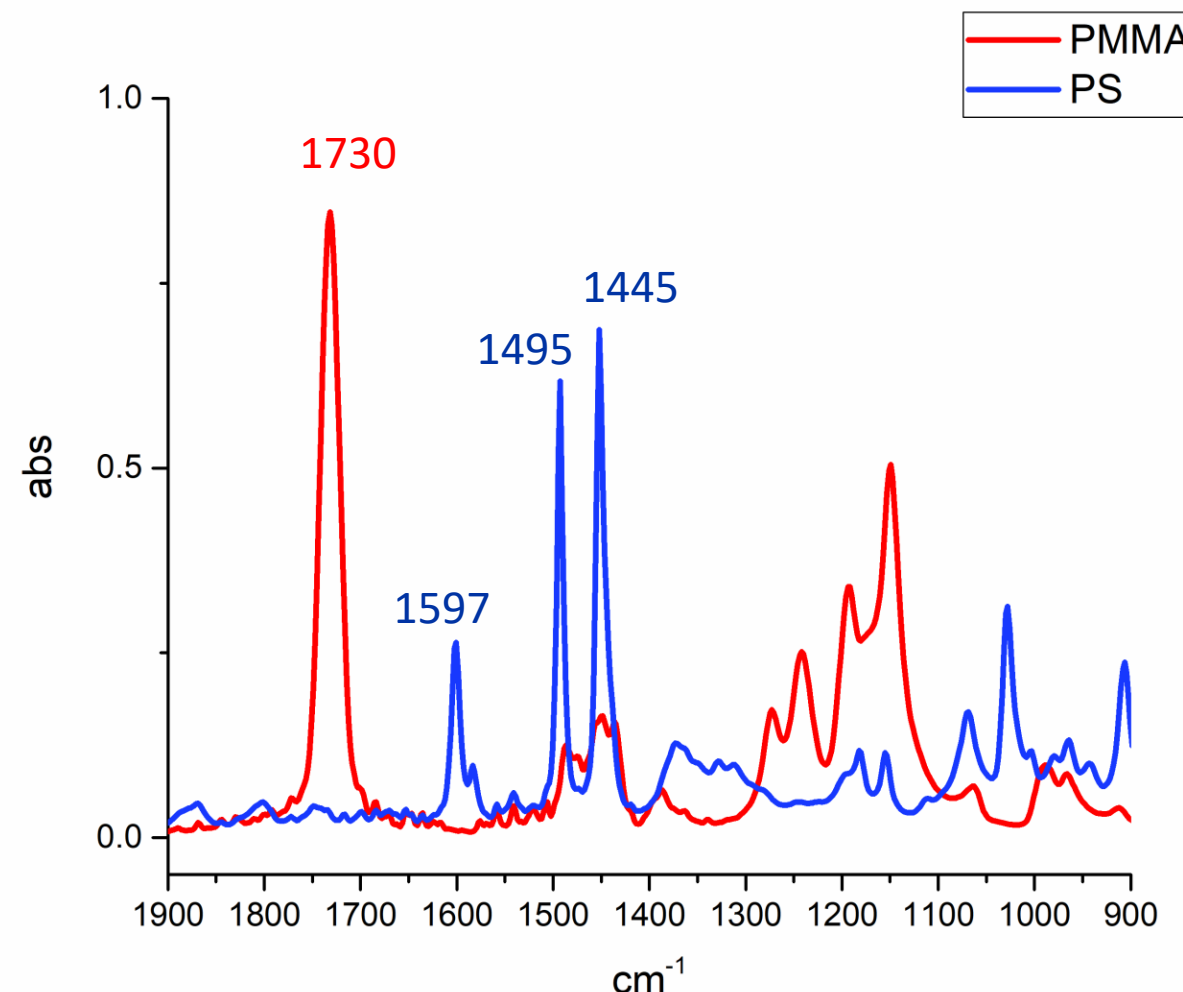
Cantilever modes

**Thermal expansion
alpha absorbance**

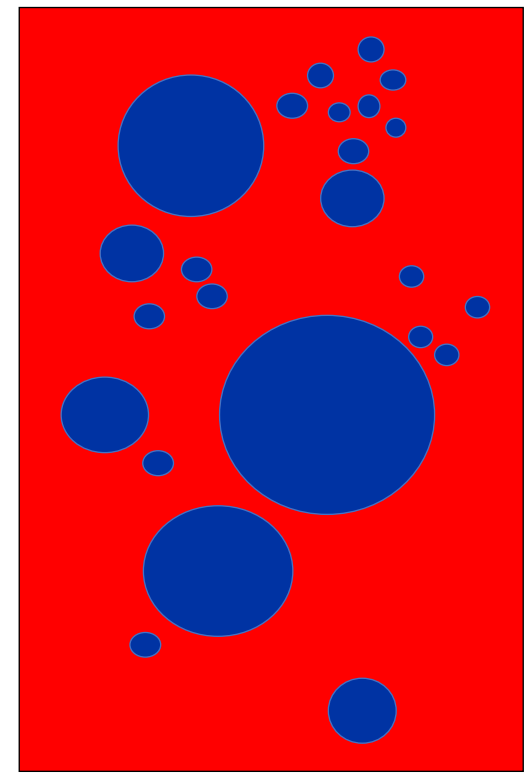
Tapping AFM-IR signal is proportional to the **absorbance** (even if non linear)

2. AFM-IR theory and concept

Examples of tapping AFM-IR results

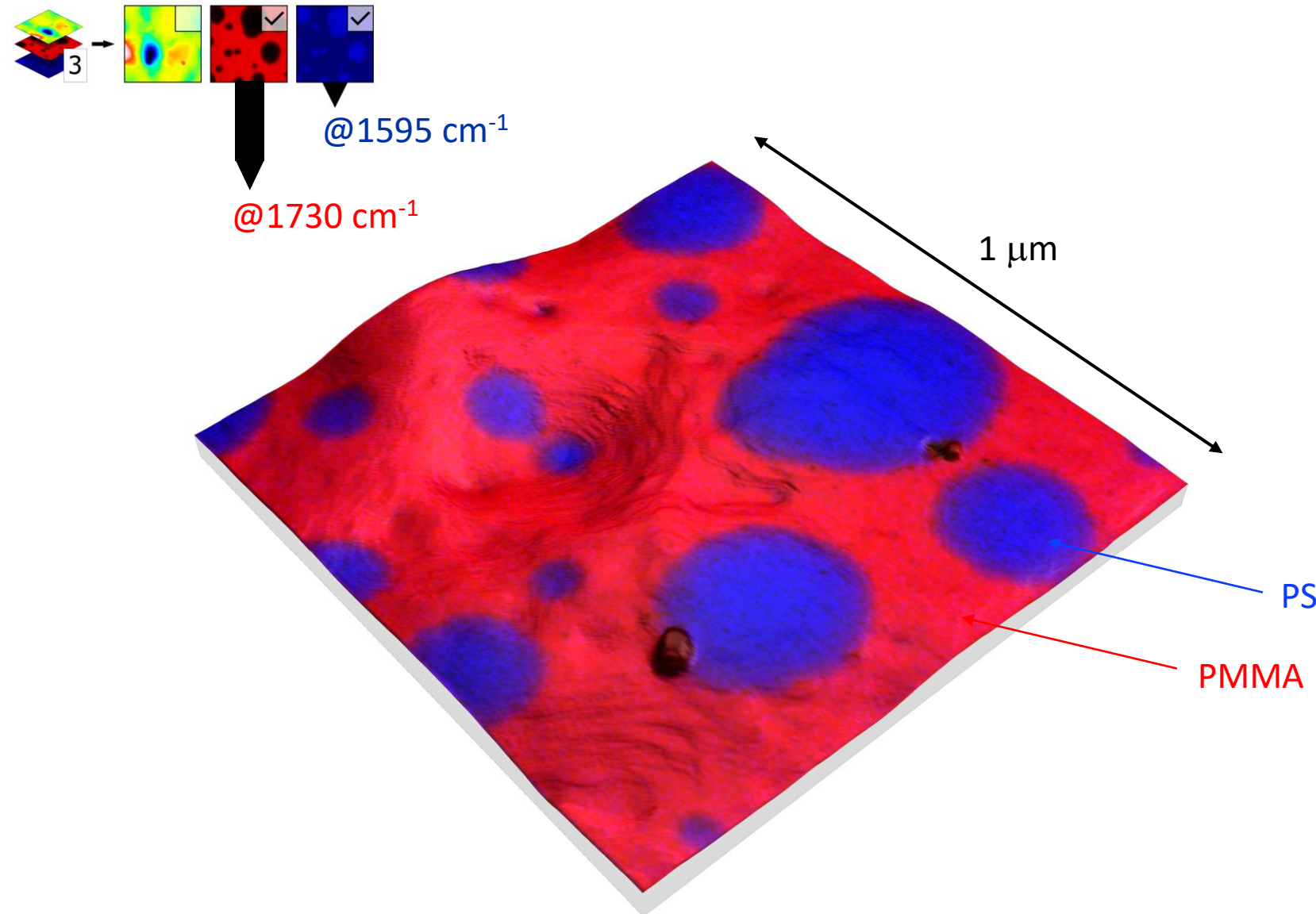


PMMA-PS polymer blend 1-1



Collab. Philippe Leclerc U-Mons

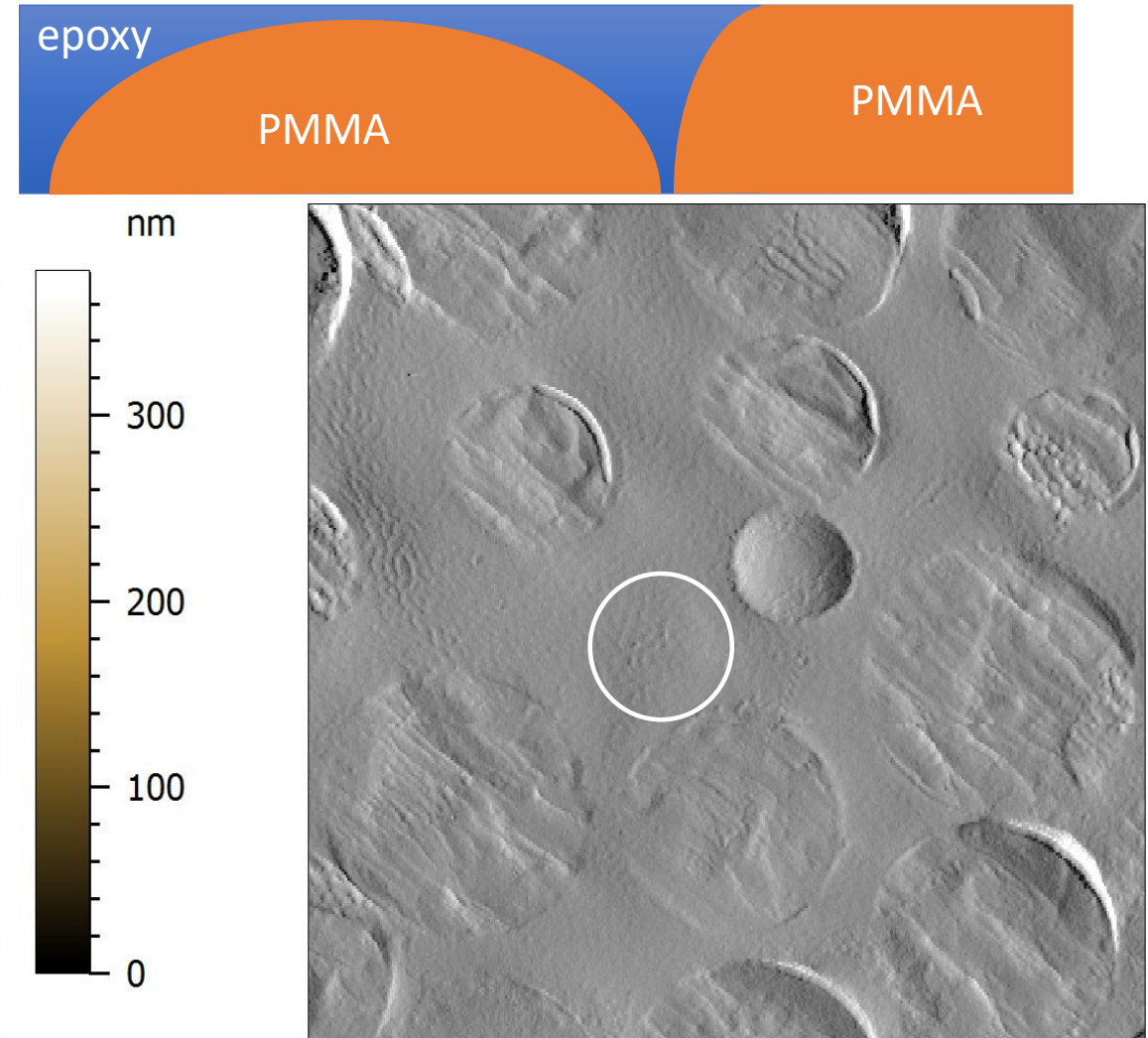
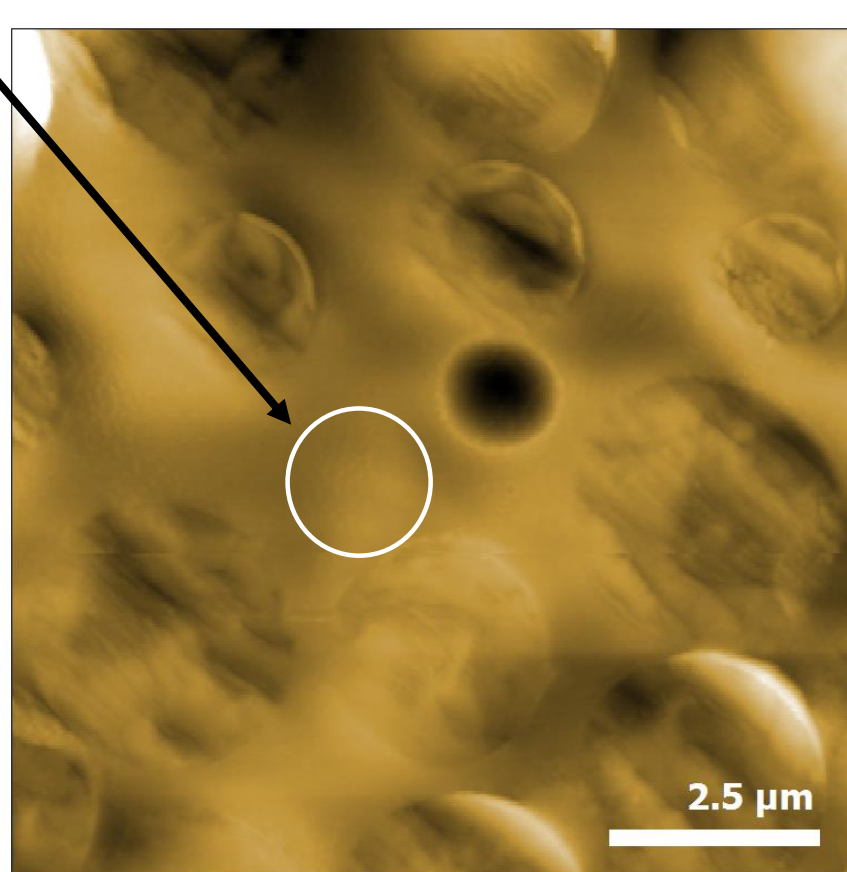
2. AFM-IR theory and concept



2. AFM-IR theory and concept

Probing depth of AFM-IR ?

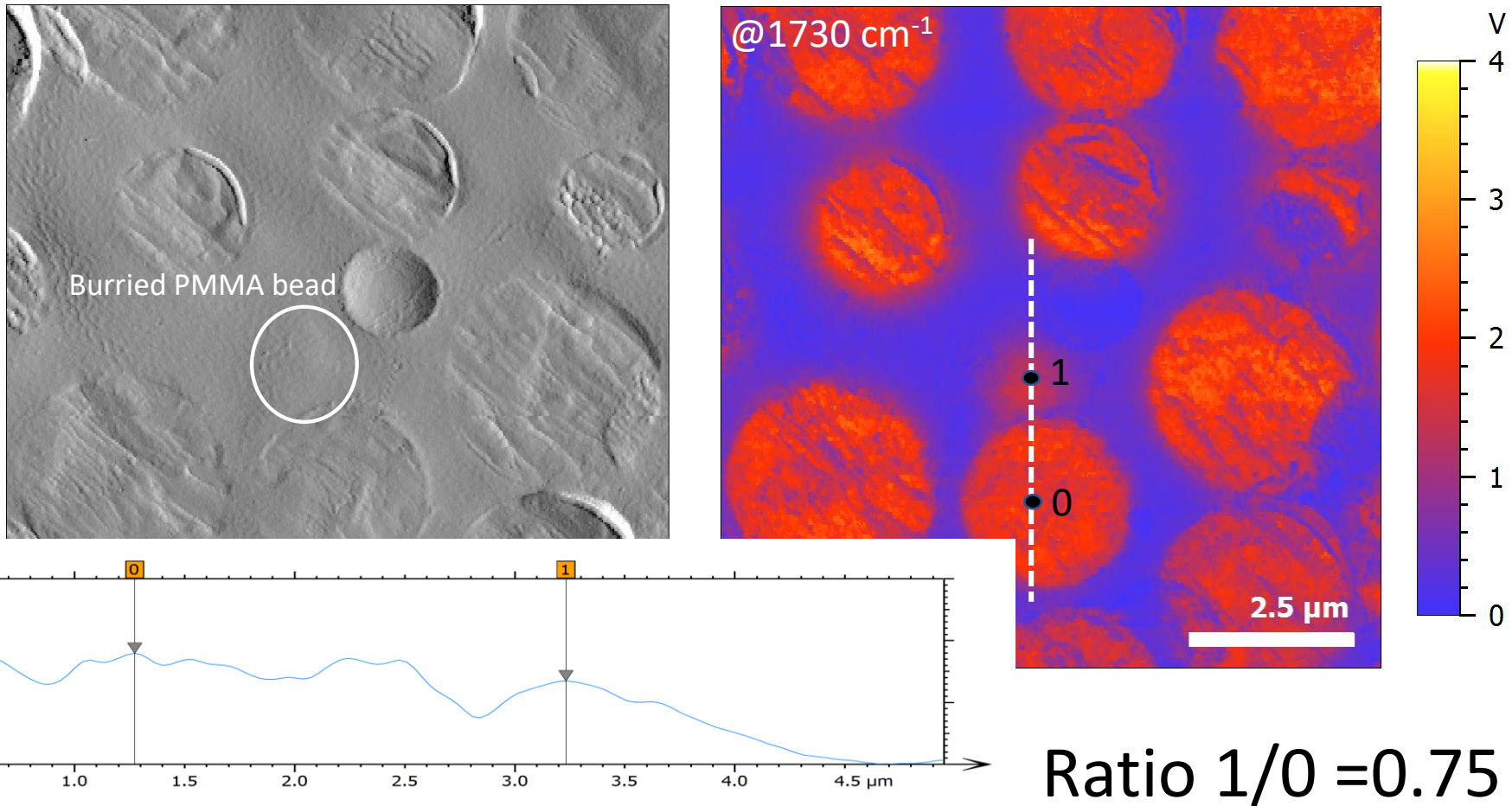
Buried PMMA bead



2. AFM-IR theory and concept

Probing depth of contact resonance AFM-IR

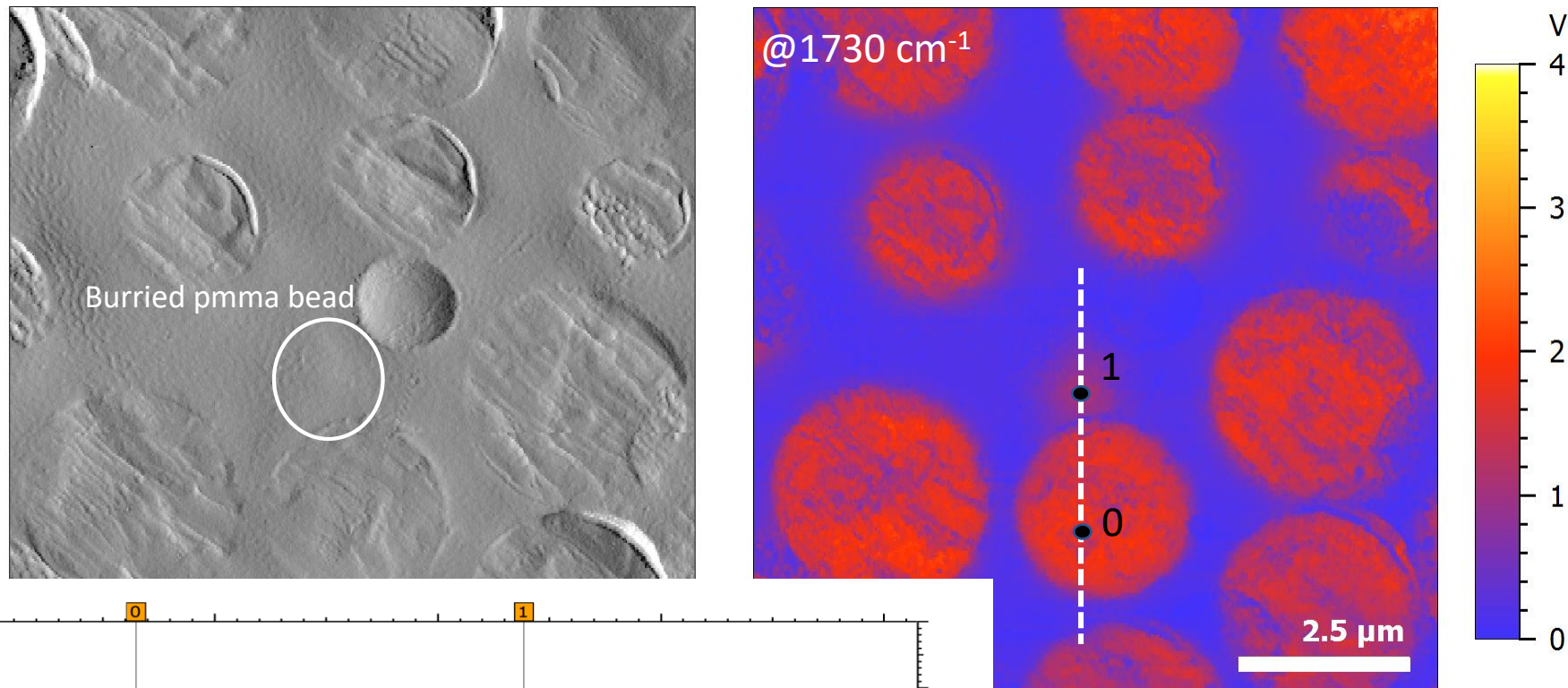
$f_{\text{laser}} = 205 \text{ kHz}$



2. AFM-IR theory and concept

Probing depth of contact resonance AFM-IR

$$f_{\text{laser}} = 550 \text{ kHz}$$

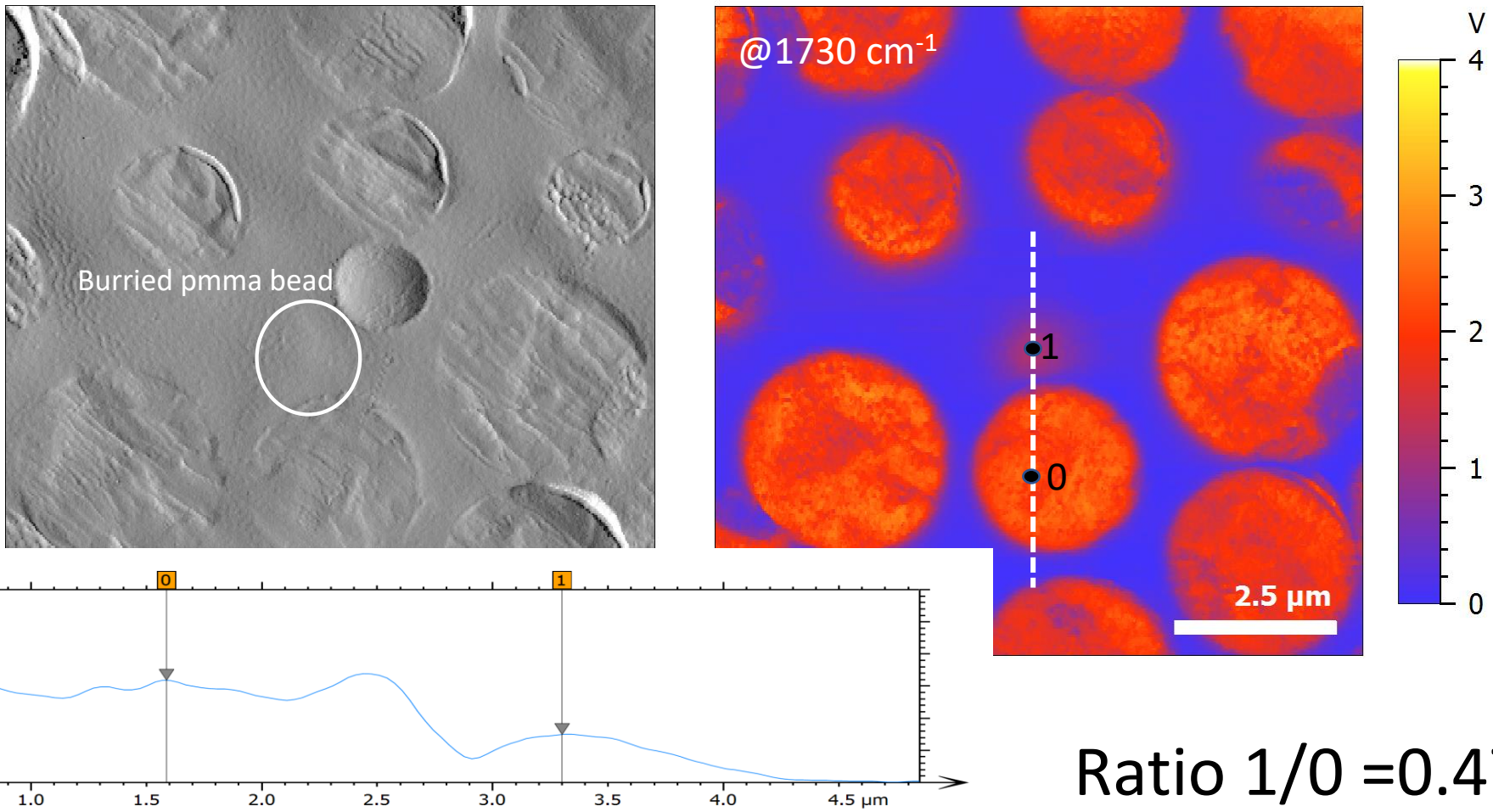


Ratio 1/0 = 0.61

2. AFM-IR theory and concept

Probing depth of contact resonance AFM-IR

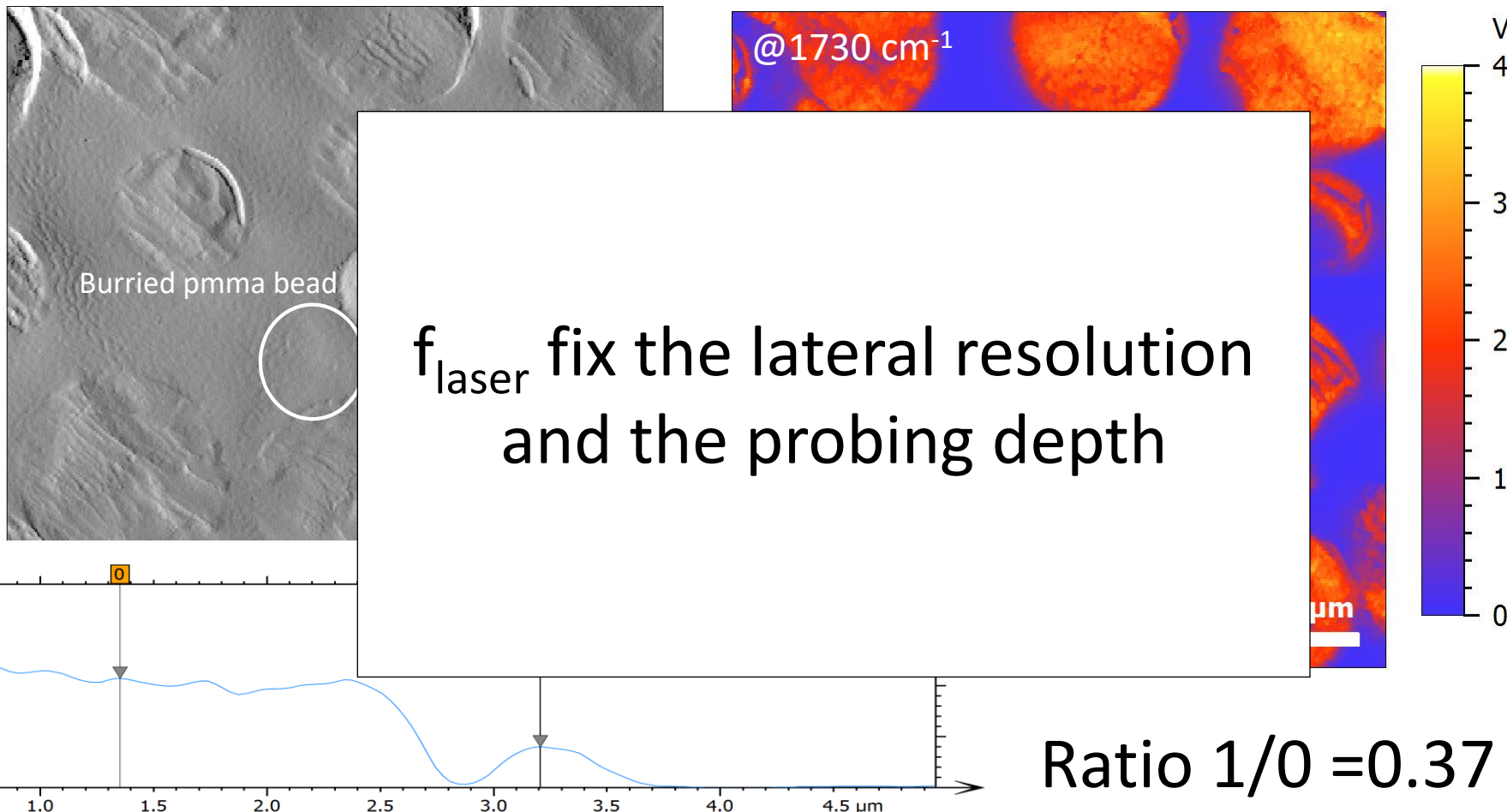
$$f_{\text{laser}} = 1250 \text{ kHz}$$



2. AFM-IR theory and concept

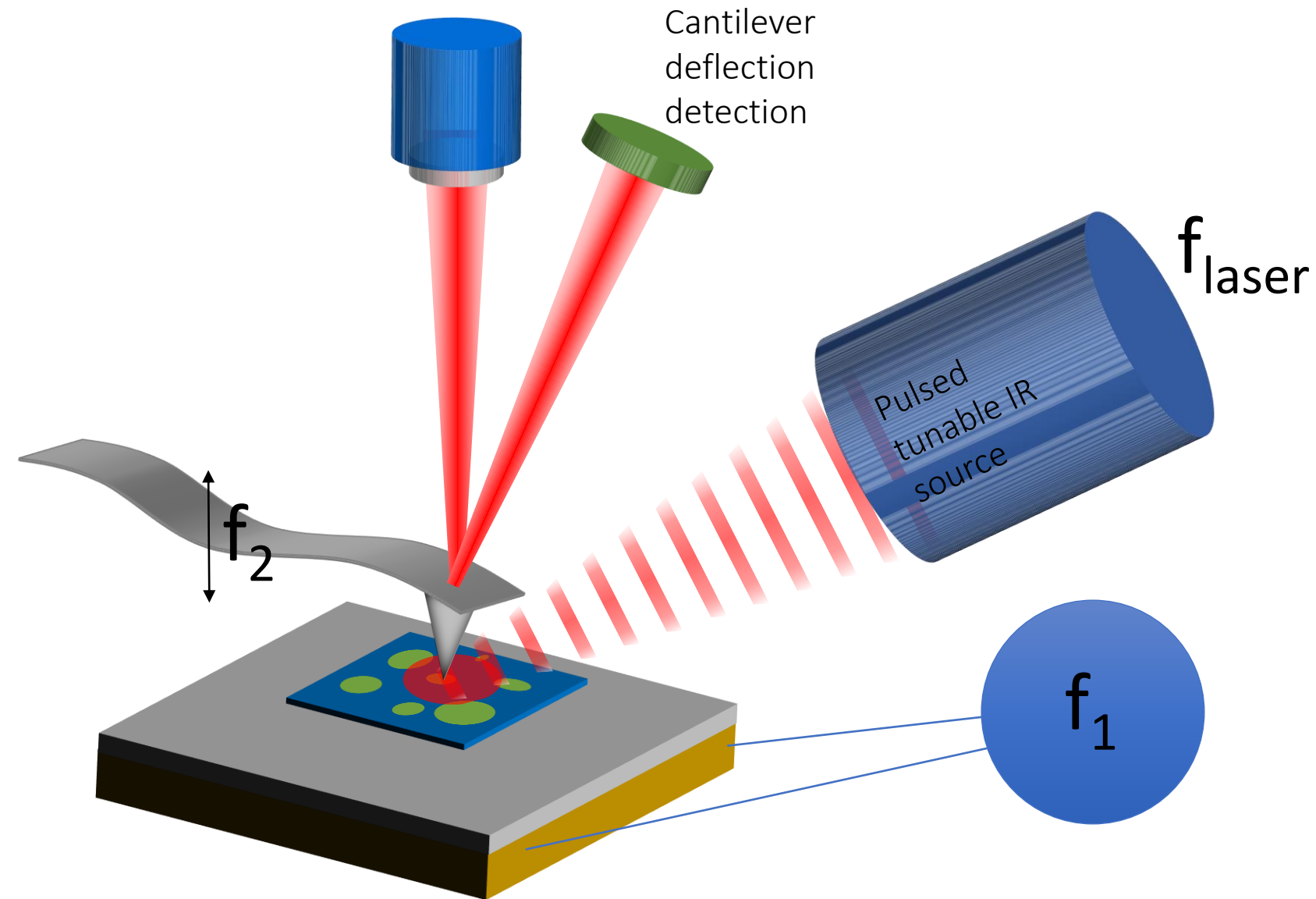
Probing depth of contact resonance AFM-IR

$$f_{\text{laser}} = 1750 \text{ kHz}$$



2. AFM-IR theory and concept

Surface sensitive AFM-IR setup



2. AFM-IR theory and concept

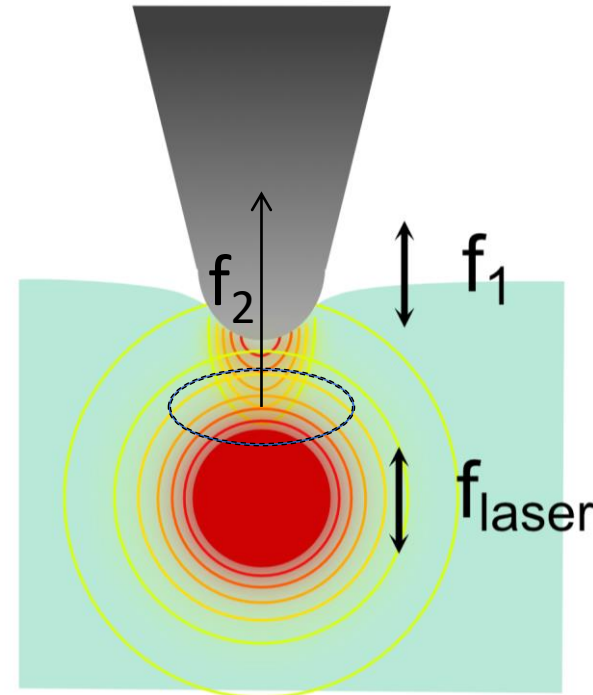
Motion equation of the cantilever mode

$$\ddot{z}_2 + \Gamma \dot{z}_2 + (2\pi f_2)^2 z_2 = \frac{1}{m^*} F_{int}(t)$$

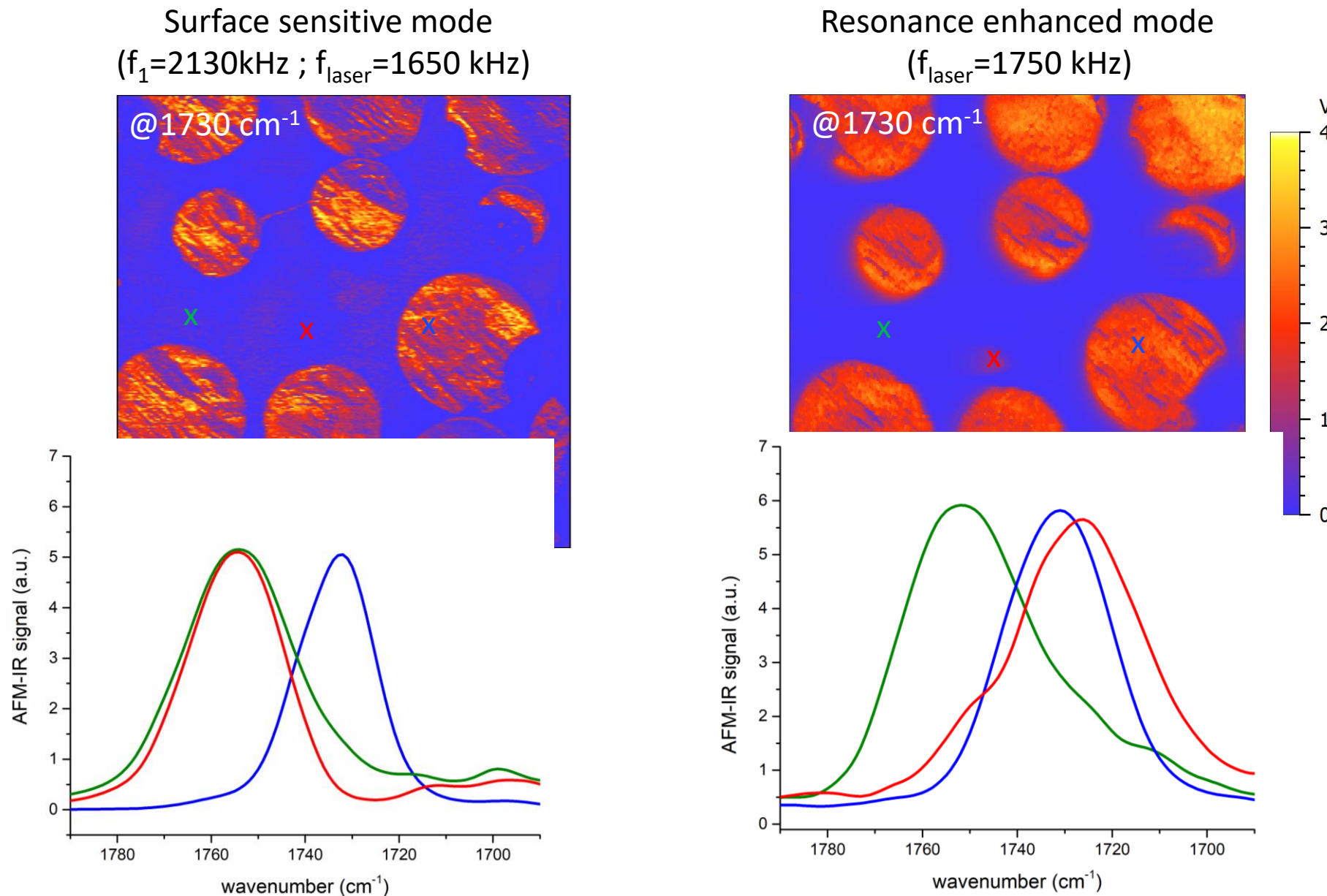
$$\begin{aligned}
 F_{int}(t) &= k_z(\delta_0 + A_1 \sin(2\pi f_1 t) - a(f_{laser}; t))^{3/2} \\
 &= k_z(\delta_0 + A_1 \sin(2\pi f_1 t) - a(f_{laser}; t)) + \chi_z(\delta_0 + A_1 \sin(2\pi f_1 t) - a(f_{laser}; t))^2 \\
 &\quad + \dots \\
 &= 2\chi_z A_1 \sin(2\pi f_1 t) a(f_{laser}; t) \quad \longrightarrow \quad \begin{aligned} &\cos(2\pi(f_1 - f_{laser})t) \\ &\cos(2\pi(f_1 + f_{laser})t) \end{aligned}
 \end{aligned}$$

Only if $f_1 + f_{laser} = f_2$ or $f_1 - f_{laser} = f_2$

$$z_2 = 2\pi^2 \chi_s \frac{Q_2}{k_c} A_1 f_{laser} t_p a_0 \quad \text{μ absorbance}$$

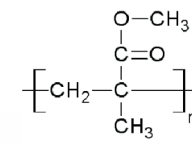
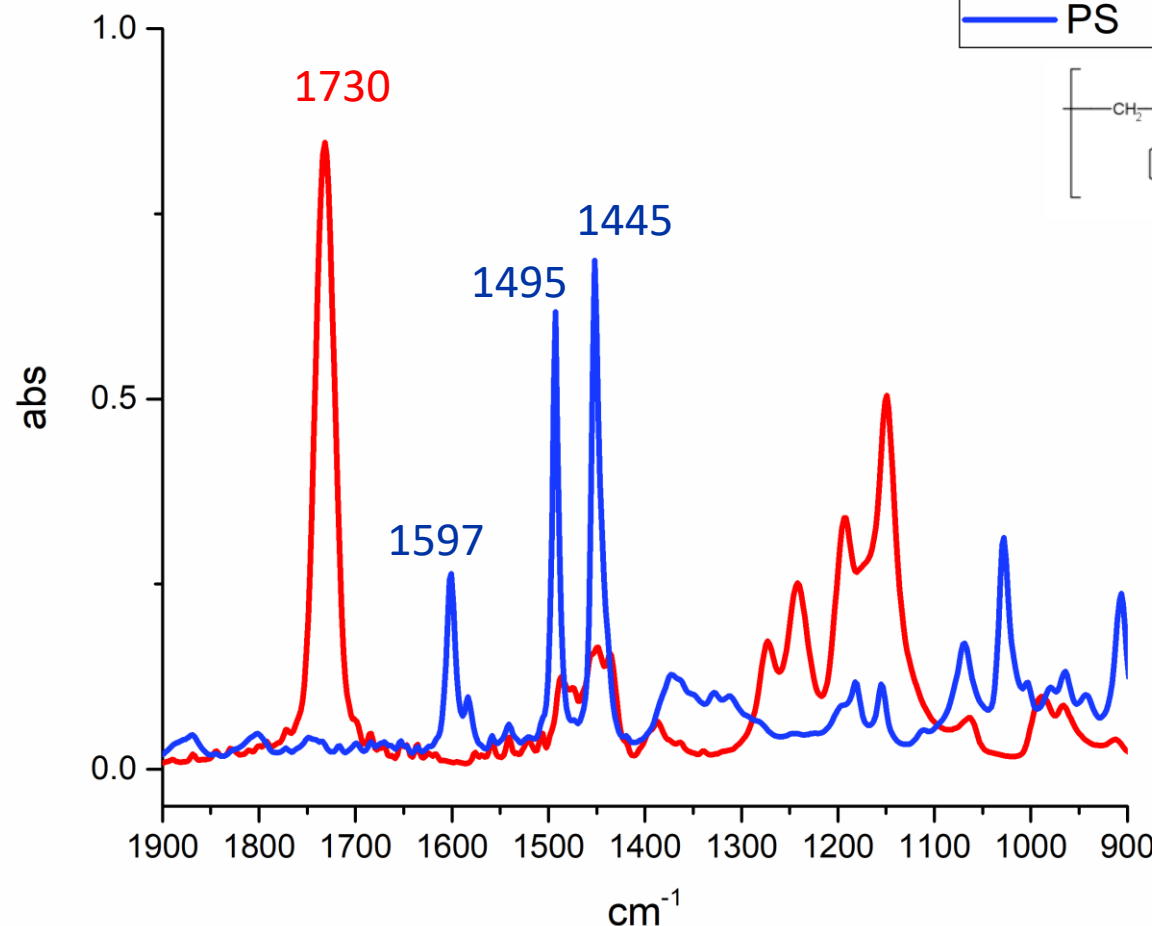


2. AFM-IR theory and concept

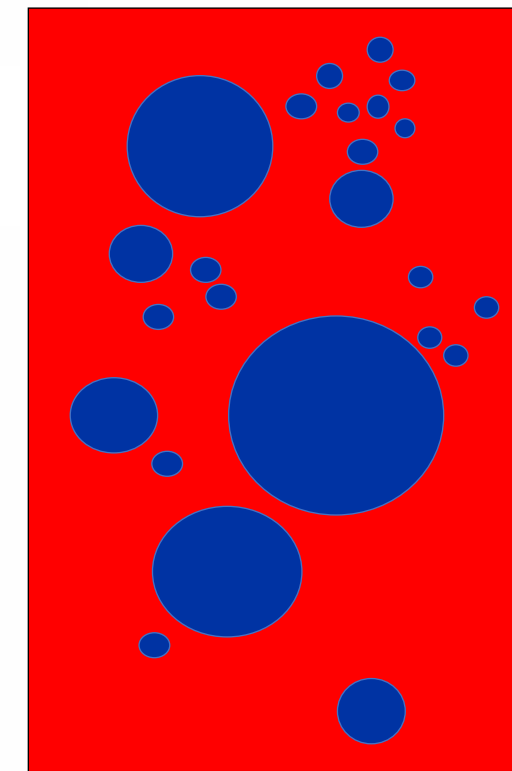
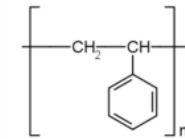


2. AFM-IR theory and concept

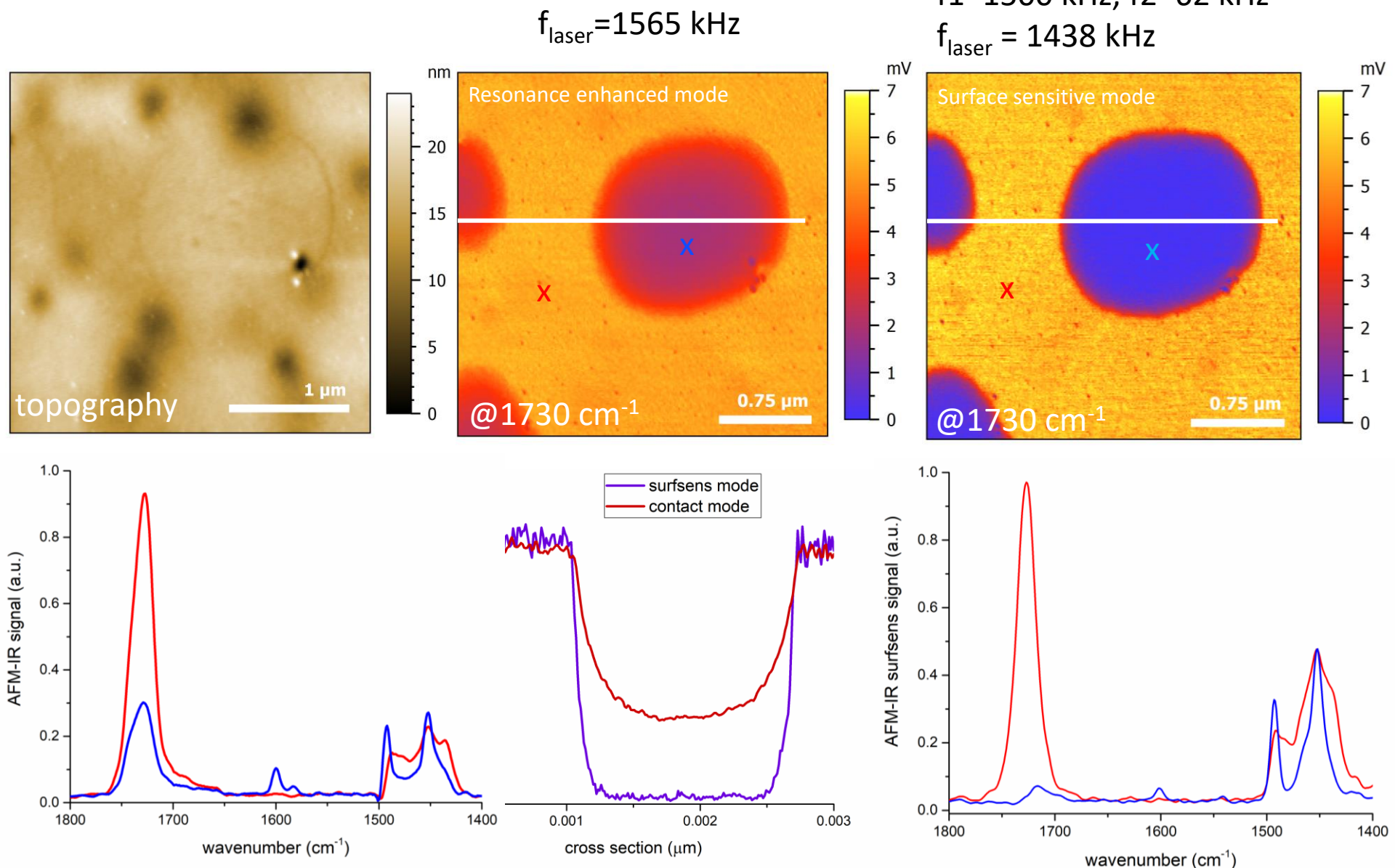
PMMA-PS polymer blend 1-1
(Philippe Leclerc , Université de Mons, Belgique)



— PMMA
— PS



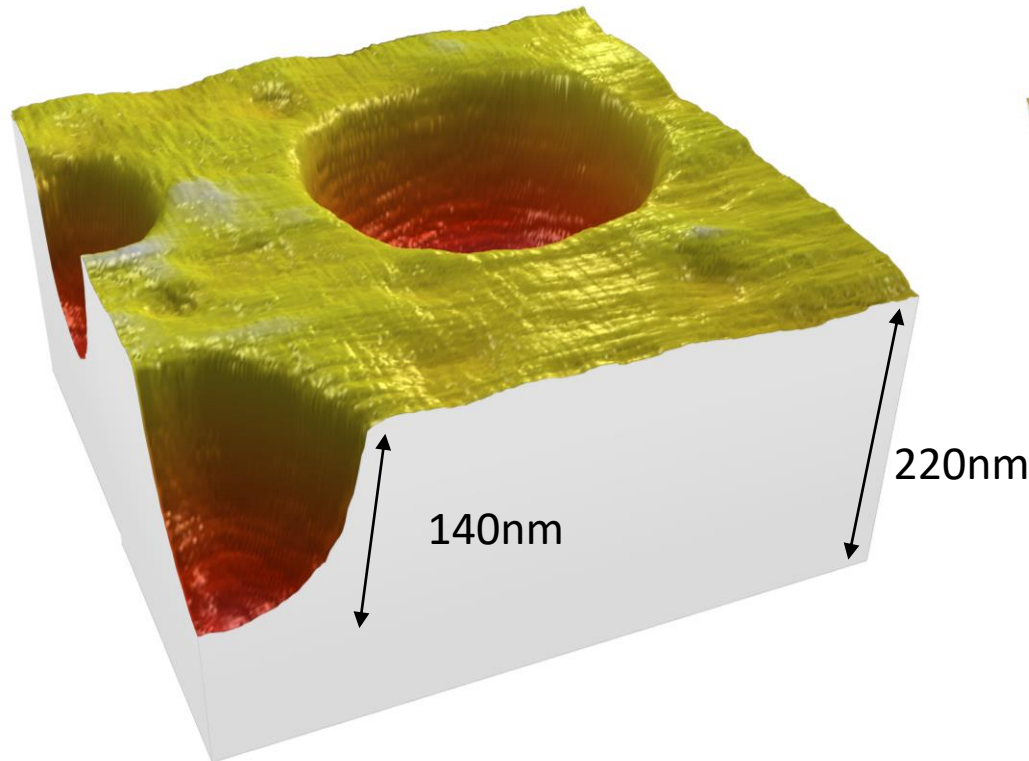
2. AFM-IR theory and concept



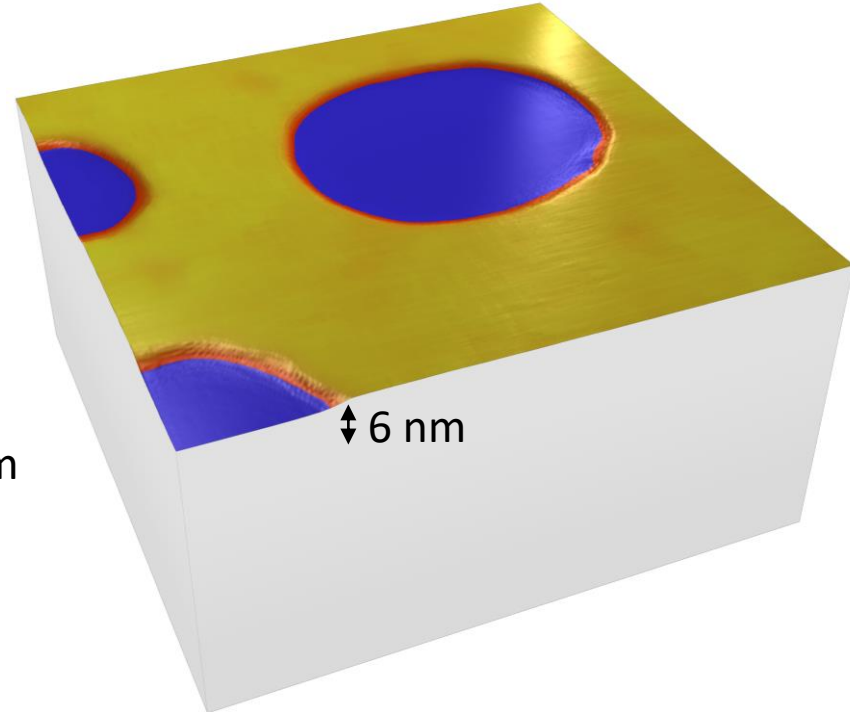
2. AFM-IR theory and concept

PMMA-PS blend

Resonance enhanced mode



Surface sensitive mode



APPLICATIONS EXAMPLES:

from bio to space via polymer and surface chemistry

« when ICON makes AFM-IR more powerfull»

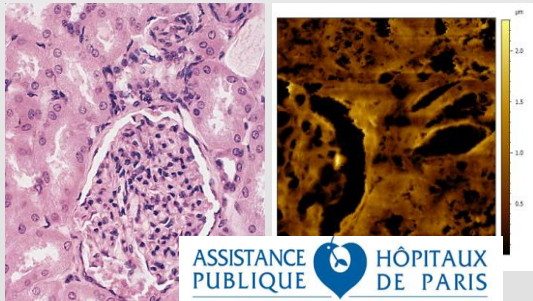
- Quality of electronics
- Mechanical and acoustic stability
- Minimum thermal drift (0.5 nm/min)



Lead to have a PLL working very well and able to correct perfectly the mechanical change during IR mapping
Better data quality with better S/N ratio, get rid of most of the artifacts, reproducability of IR maps.

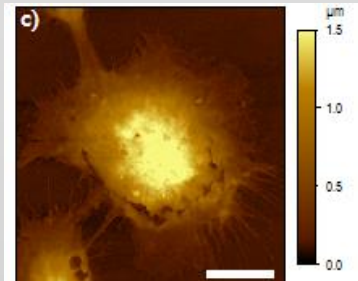
Field of applications - Biology

TISSUE – Human cells



ASSISTANCE PUBLIQUE HÔPITAUX DE PARIS

Calcification in human tissues
Extracellular vesicles
Penetration of nanocarriers



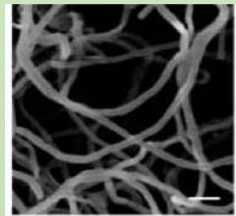
Nanoparticules and cell:
macrophage

L'ORÉAL

Fine structure of the hair...

MICRO-ORGANISMS

Accumulation of biopolymer or lipids



Localisation and quantification

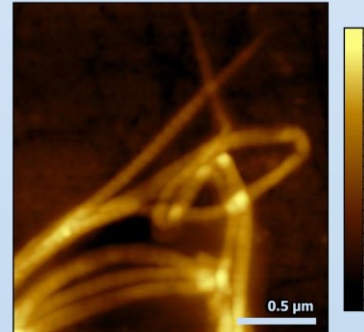


Local composition, TAG, DAG, MAG
and FFA differentiation



NANOMETRIC SCALE

Protein assemblies



Collagen fibrils denaturation
System complex: Collagen-
antibiotic



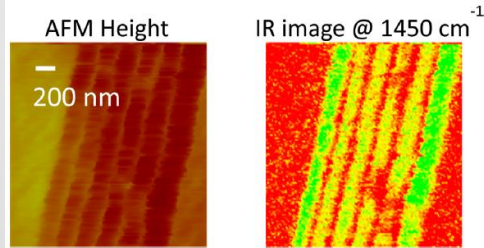
Bacterial amyloids
Beta structure of amyloids
Prion, lipids bilayer



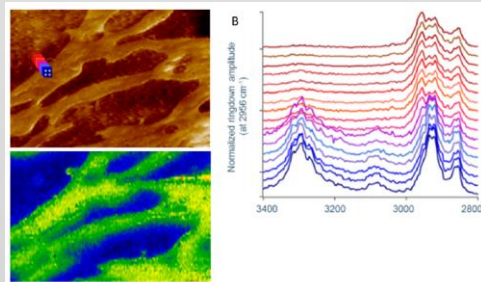
Field of applications

Polymers sciences

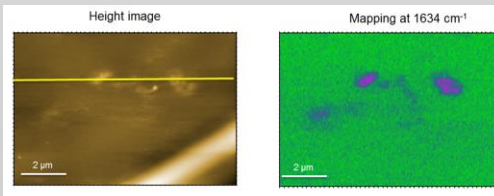
Multilayers:
Structure-cristallinity



A Dazzi, Chem Rev, 2016



Trace of adjuvant blooming



A Dazzi, International journal of pharmaceutics Volume 484, Issues 1–2, 2015

Heritage sciences

- Investigate
parchments
degradation



G.Latour, Scientific Report, 2016

- IR signatures: heterogeneities in
ancient tissues or violin sections

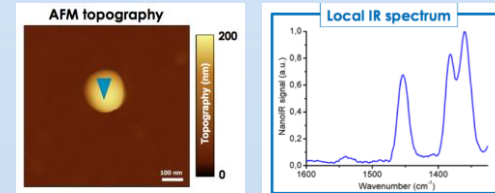


IPANEMA | ARCHAEOLOGY CONSERVATION SCIENCES
PALAEONTOLOGY PALEO-ENVIRONMENTS

ANCIENT MATERIALS
RESEARCH PLATFORM

Nanoparticles

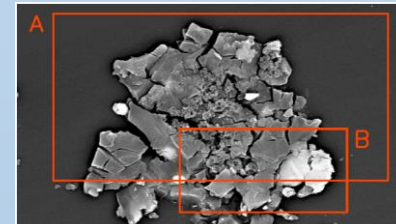
- Polymeric Nps



Mathurin J., 10.1039/C8AN01239C, Analyst, 2018

Astrochemistry

- Investigation of organic
matter in micrometeorites

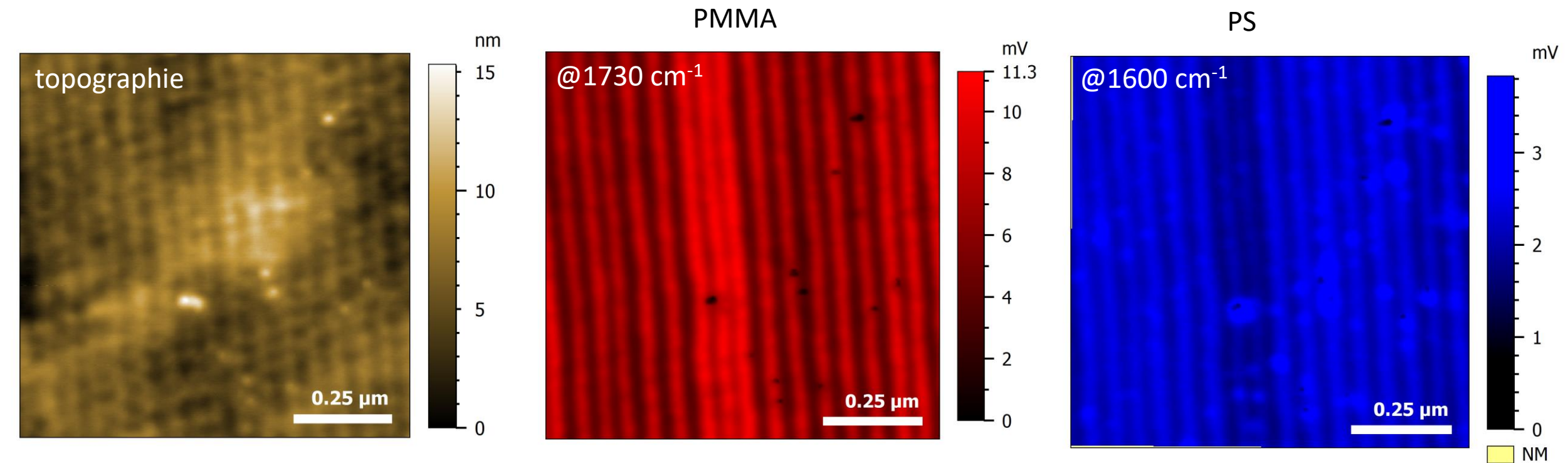


CSNSM
Centre National de la Recherche Scientifique

J. Mathurin, A&A, 2019

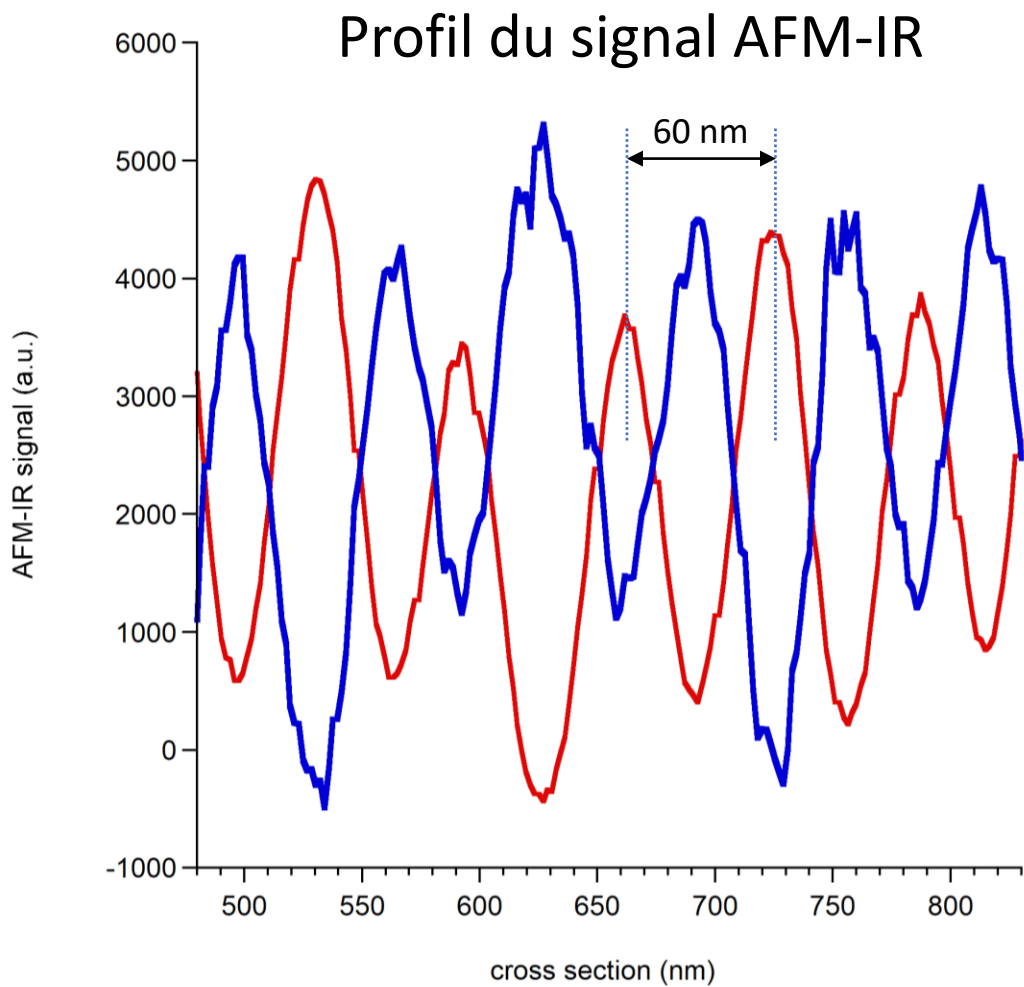
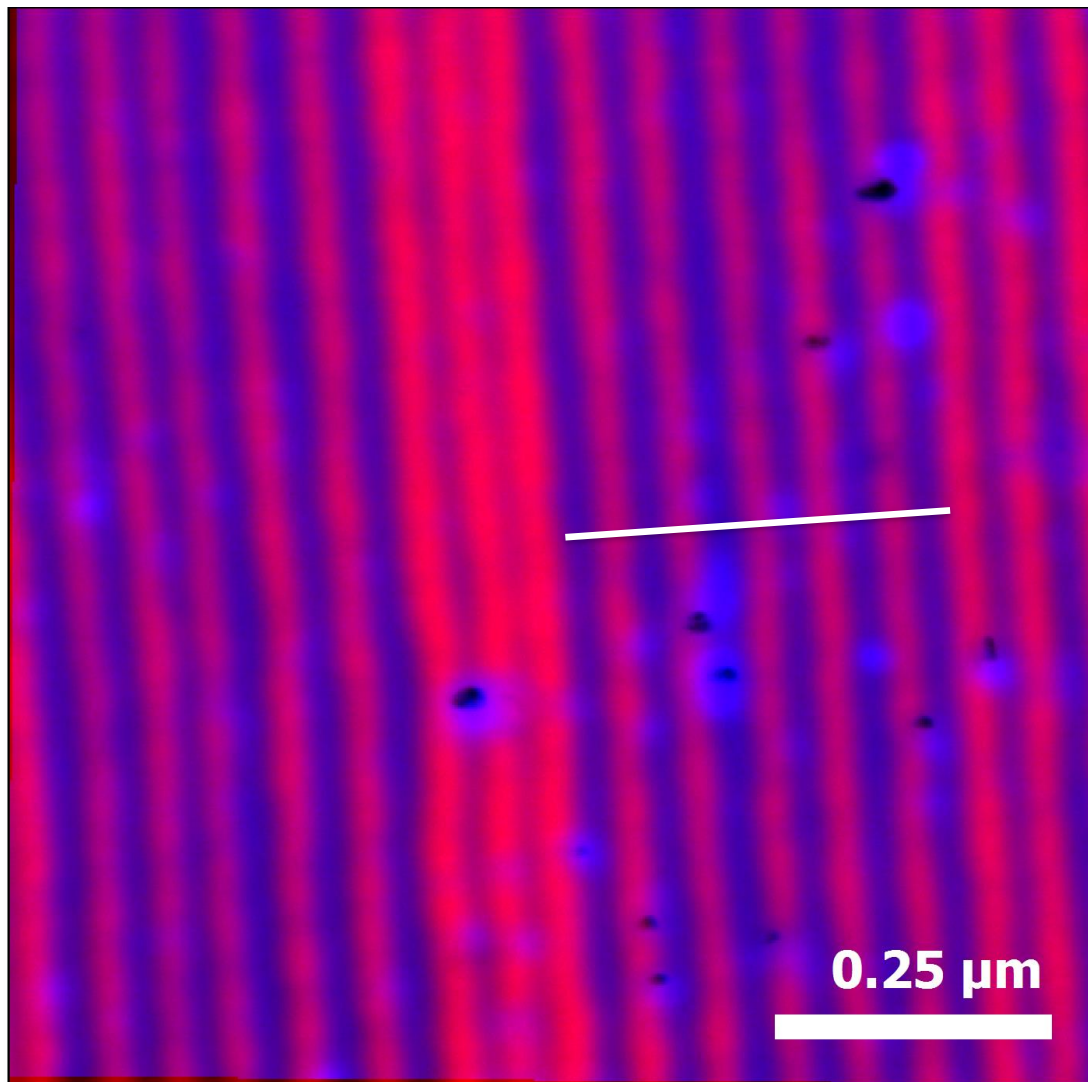
3. Applications examples

PS-PMMA multi-layers film



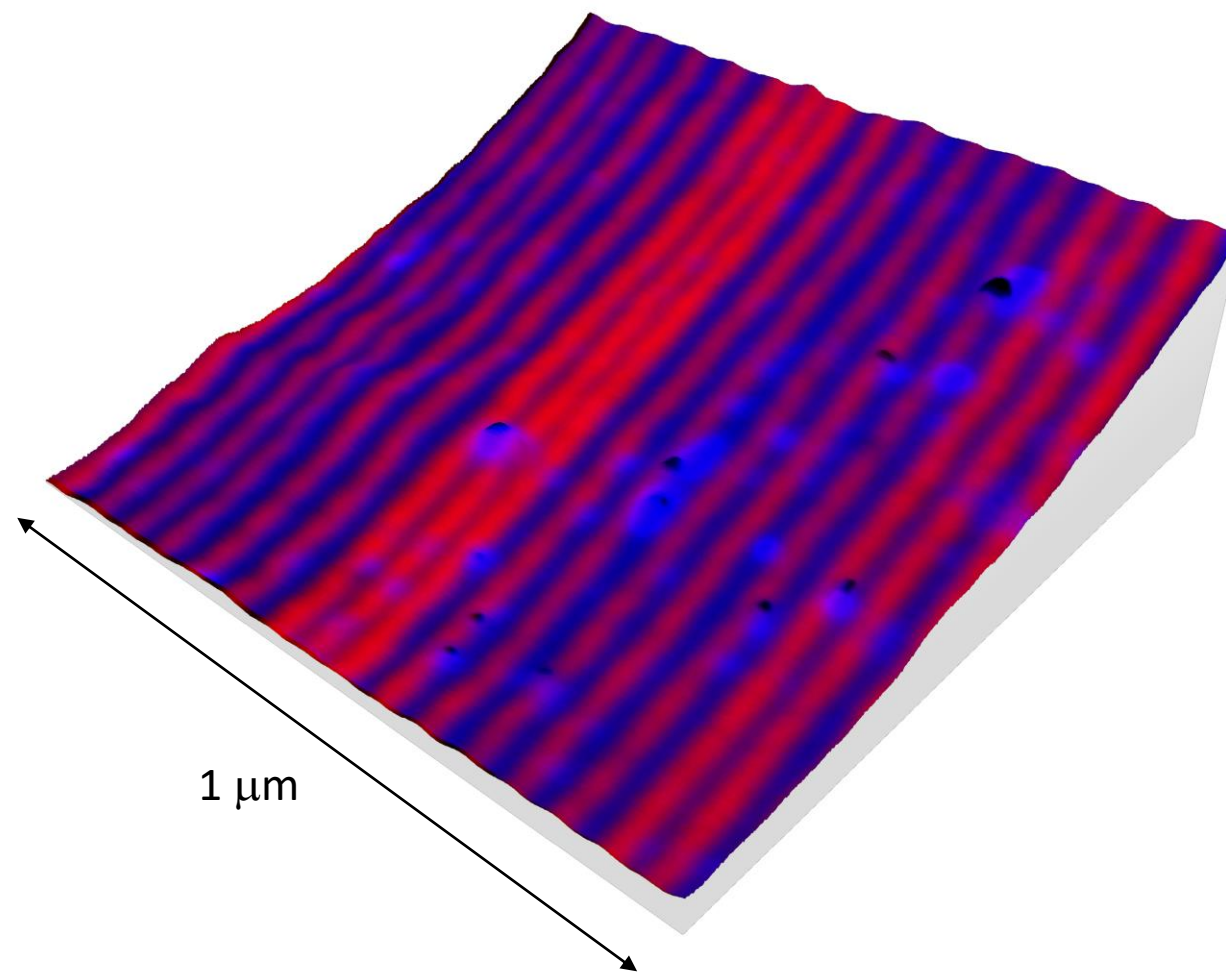
3. Applications examples

Overlay imaging (1730 and 1600)



3. Applications examples

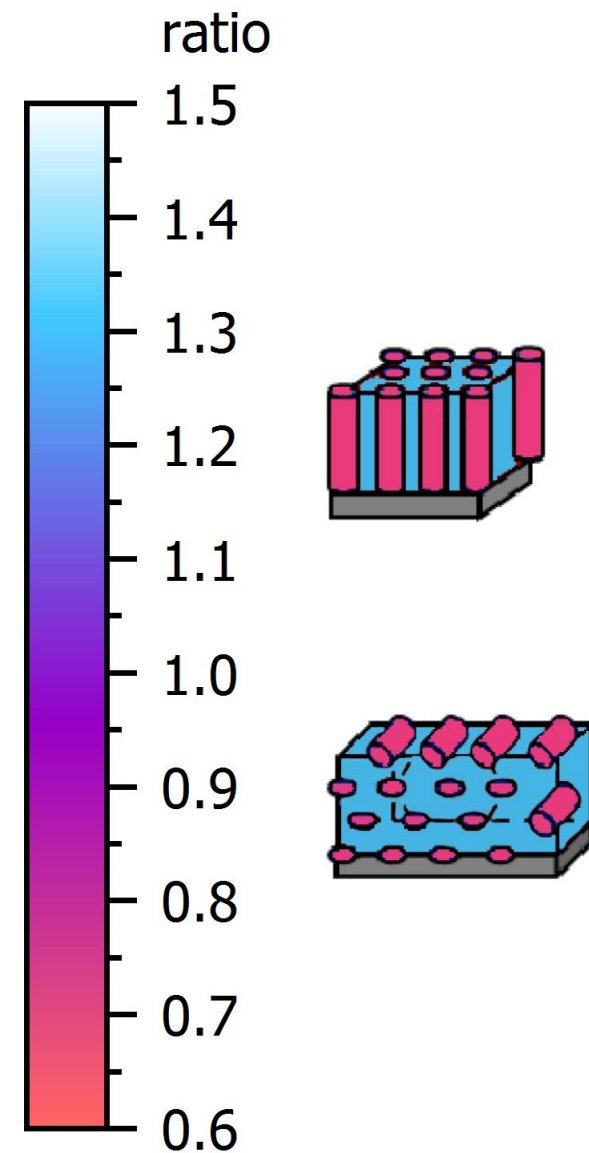
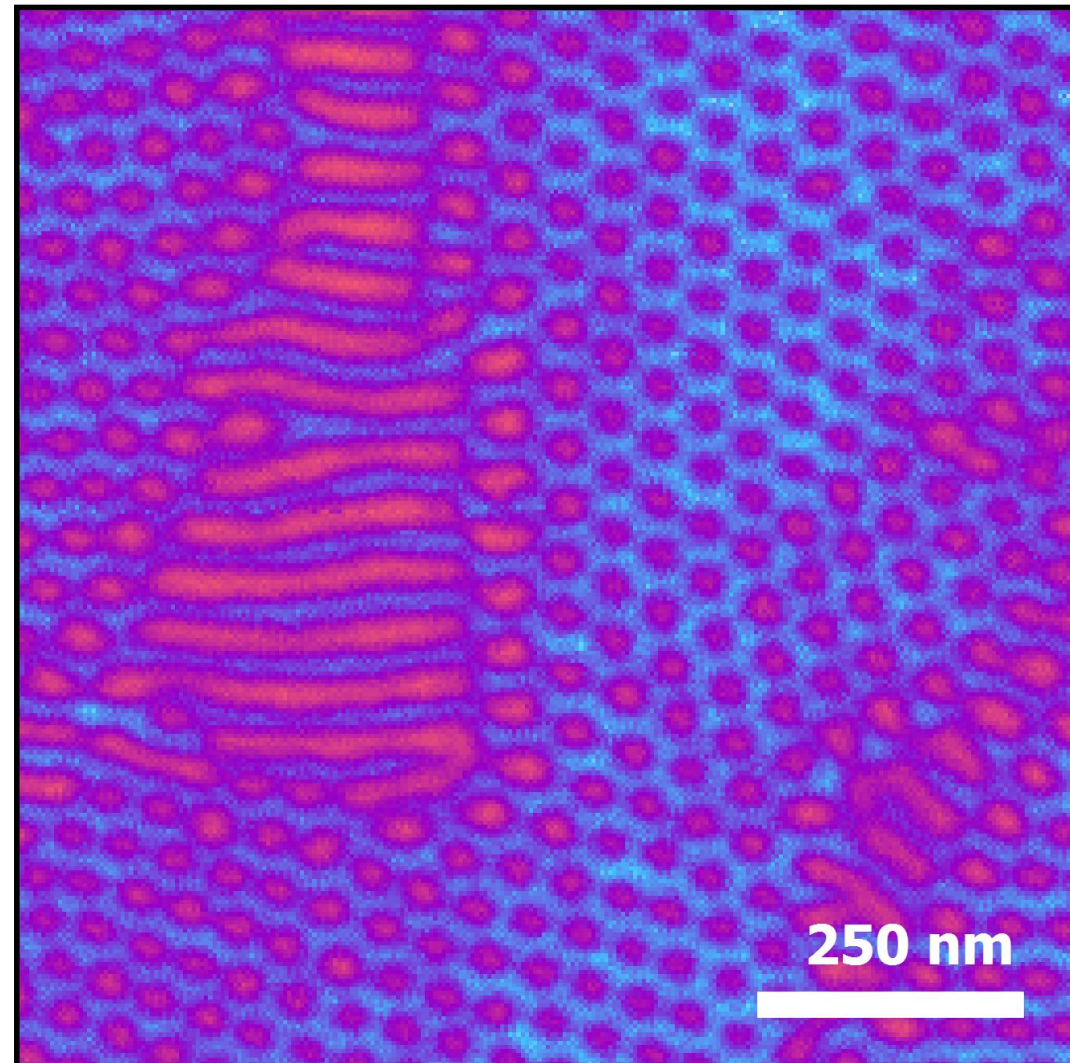
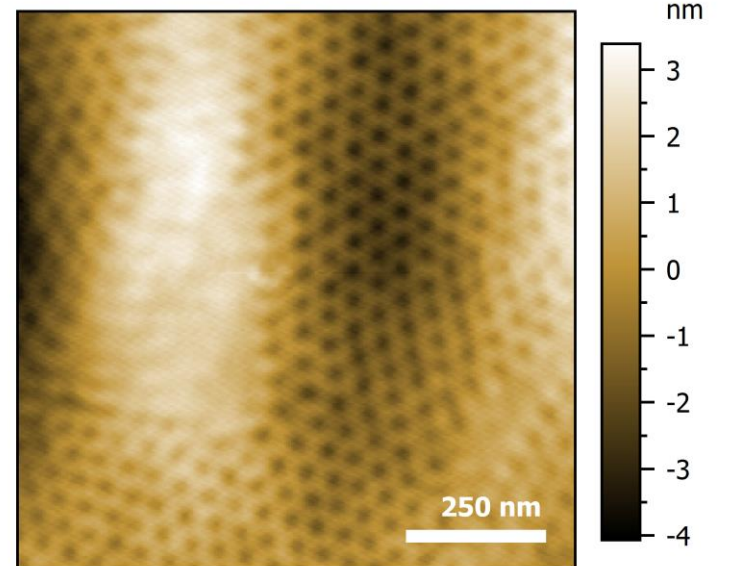
3D overlay imaging



3. Applications examples

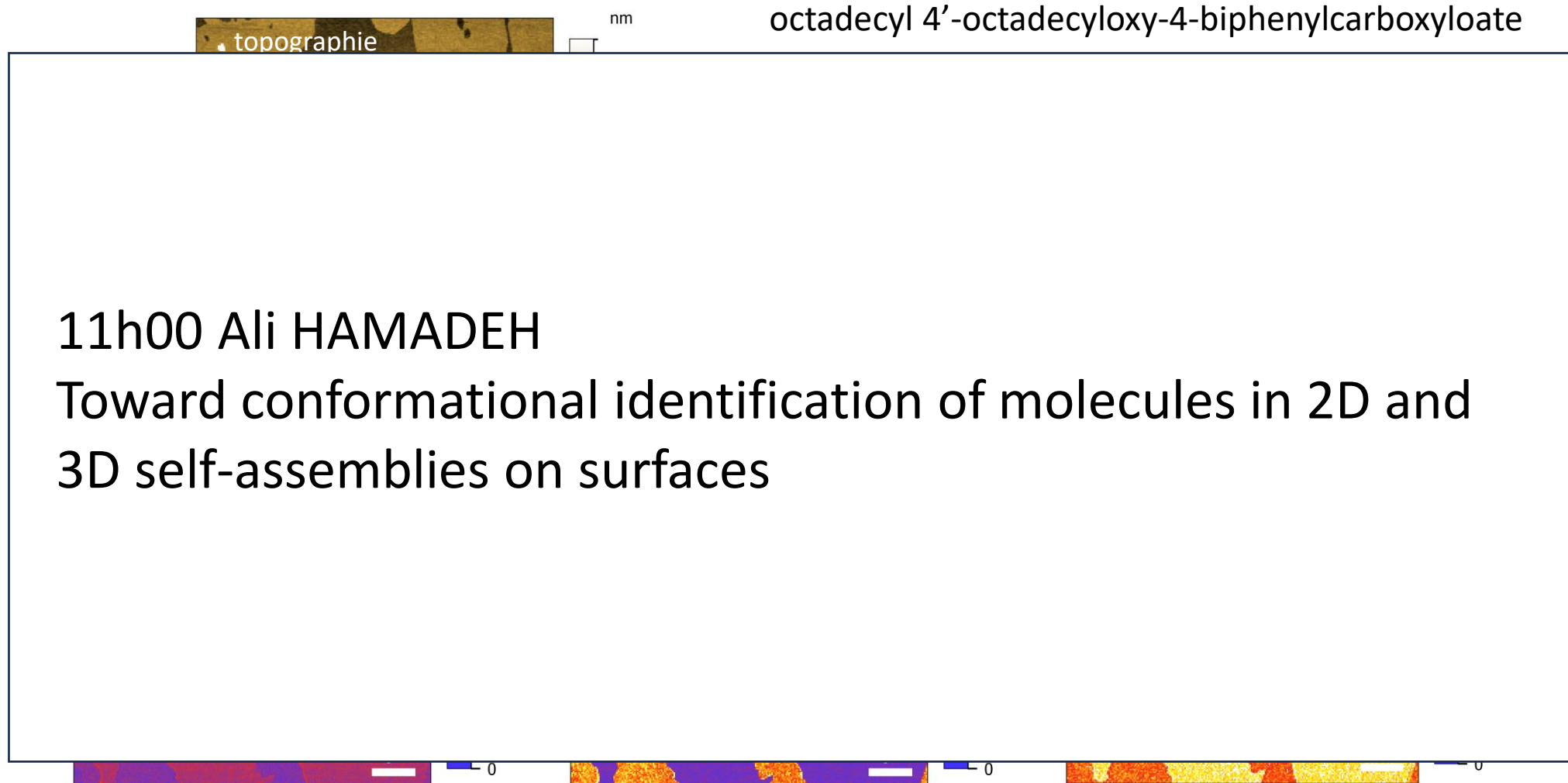
Structuration of PLA/PS copolymer

topography

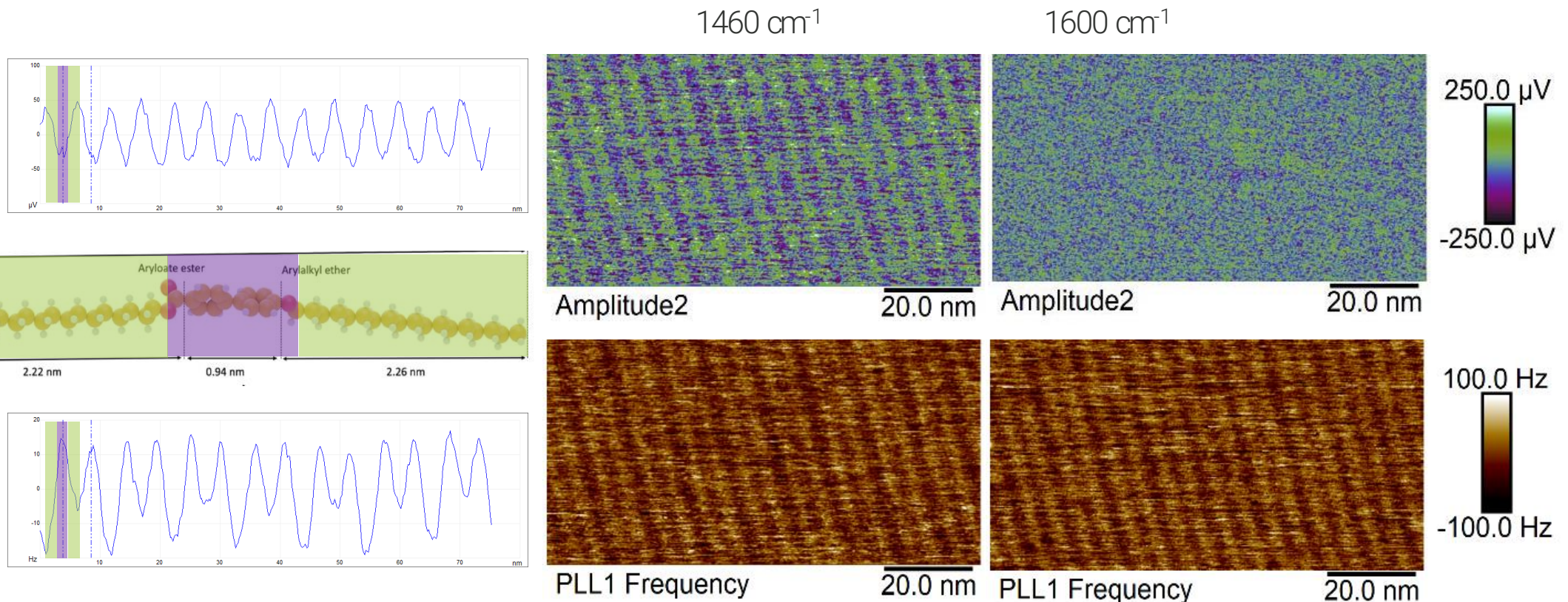


3. Applications examples

Molecular monolayer (OC18) on HOPG



3. Applications examples



- Resolution: **1-2 nm** (10-90% ‘level’)
- Monolayer (0.8 nm) sensitivity on HOPG
- Low drift: < 0.2 nm/min

Collaboration with

- Dr. Peter Dewolf (Bruker)
- Pr. Frank Palmino (Université de Franche-Comté, FEMTO-ST)
- Dr. Frédéric Chérioux (CNRS, FEMTO-ST)

3. Applications examples



Hayabusa2 spatial mission

R

20
matter,

11h40 Jérémie MATHURIN

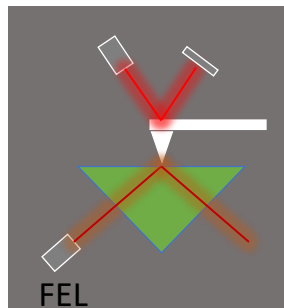
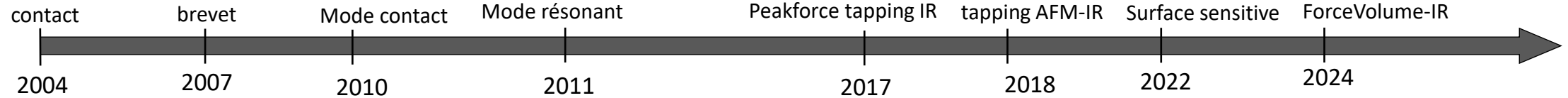
Caractérisation à l'échelle nanométrique par AFM—IR des échantillons de la mission spatiale japonaise Hayabusa 2

200

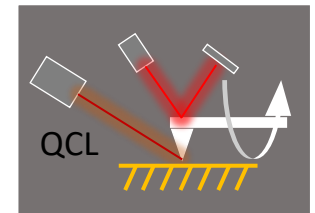
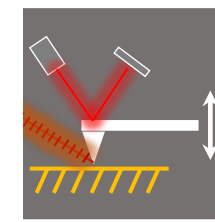
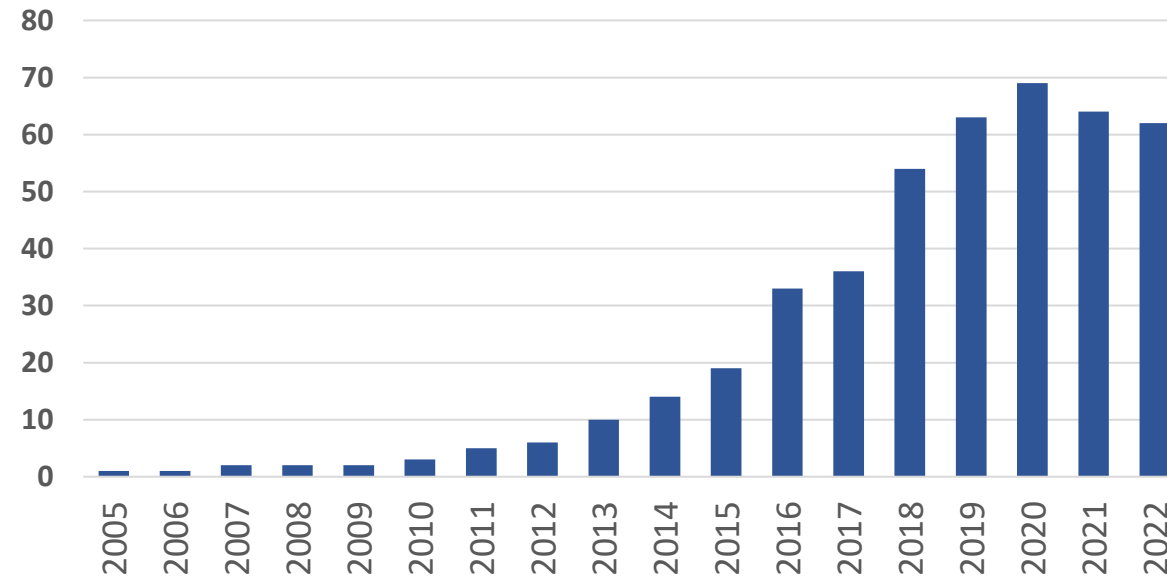


5 mm

4. Evolution of the AFM-IR technique



Articles AFMIR (nov. 2022)

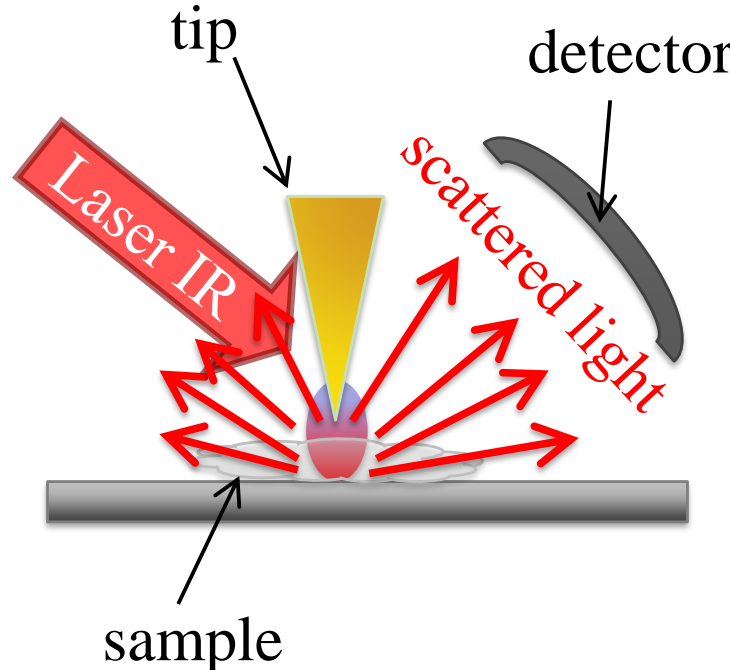


80% of nanoIR paper

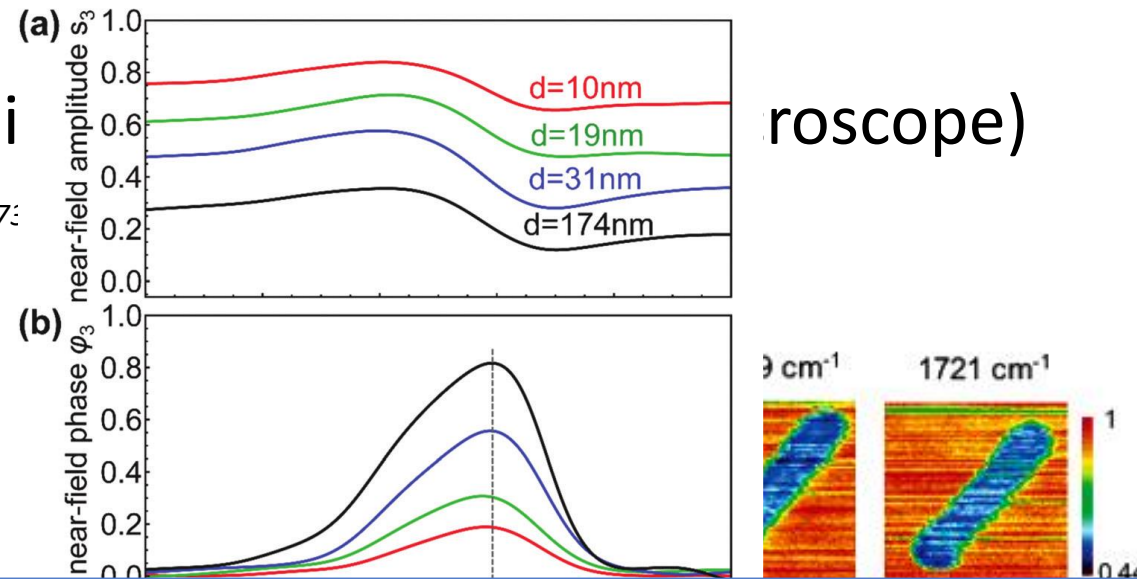
5. Comparison with competitors

- Scattering SNOM (Scanning Near-field Optical Microscopy)

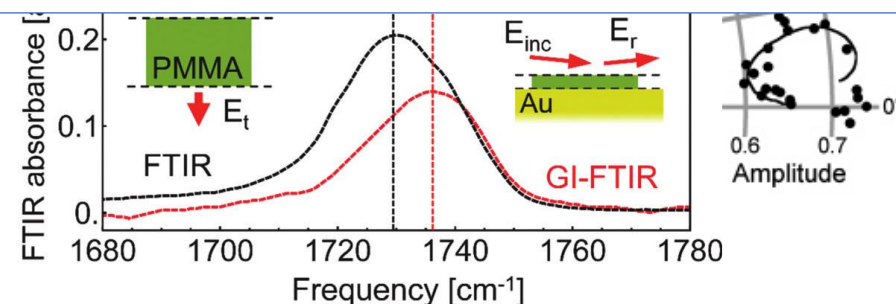
B. Knoll and F. Keilmann, Nature, Volume 399, Issue 6733, 1999



scope)



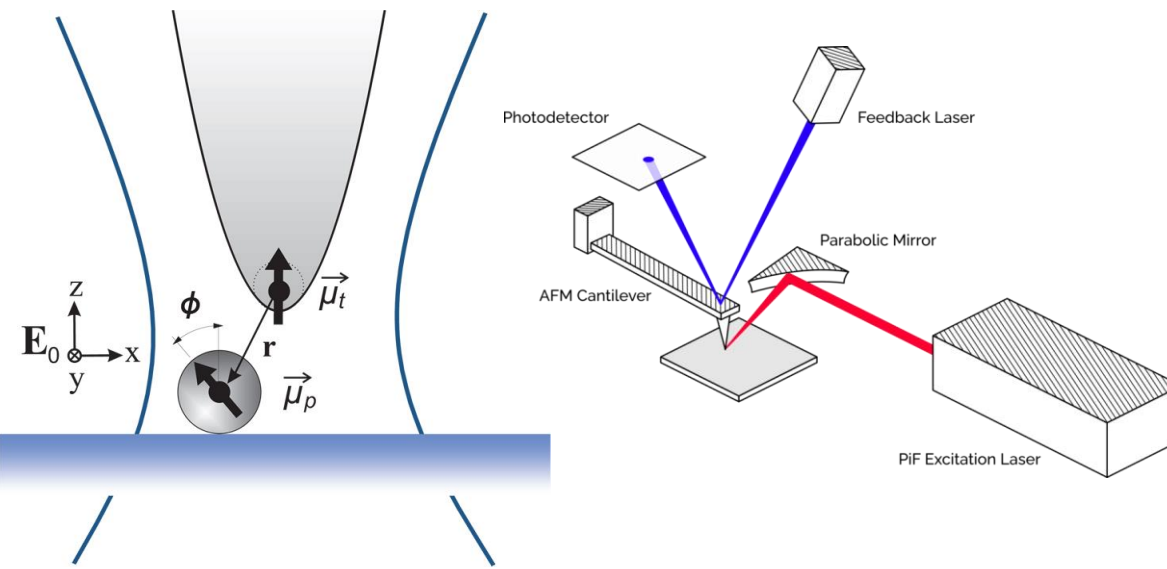
$$\text{Signal}(x, y) = \alpha(x, y)\text{Re}(n) + \beta(x, y)\text{Im}(n)$$



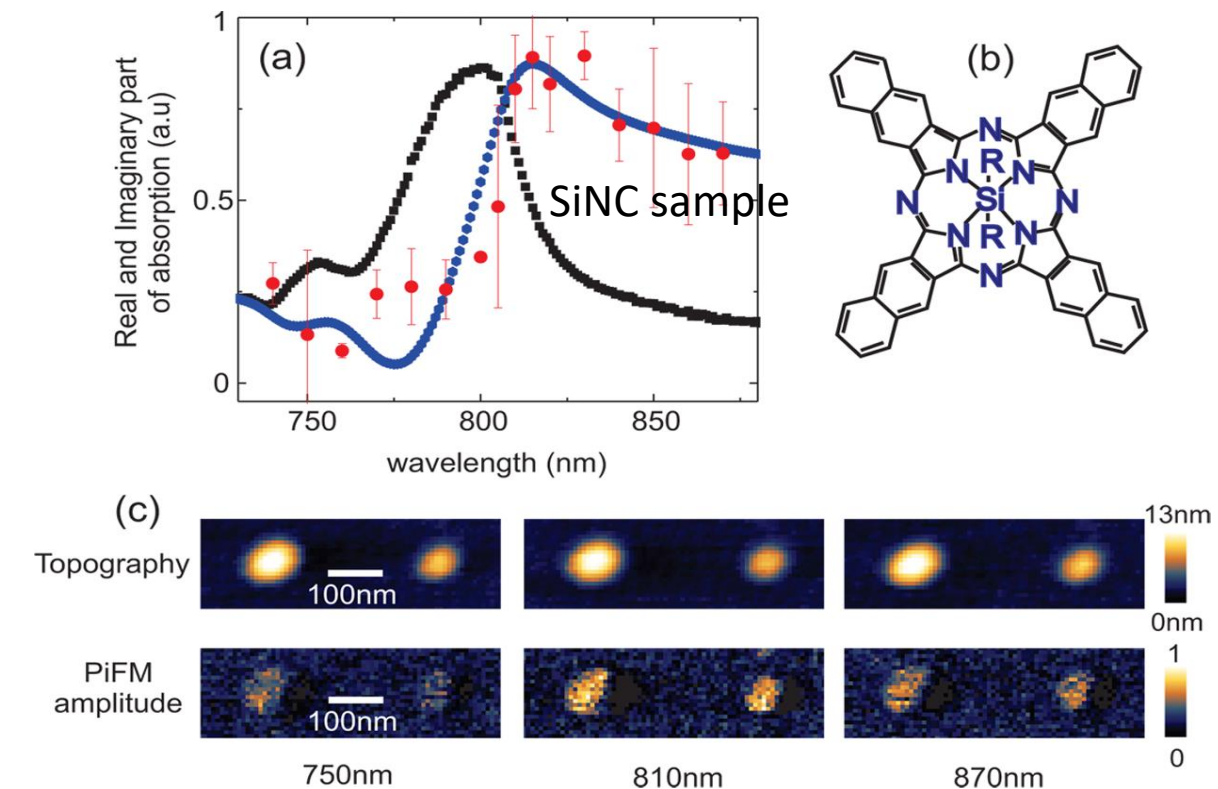
5. Comparison with competitors

- PiFM (Photo-Induced Force microscope)

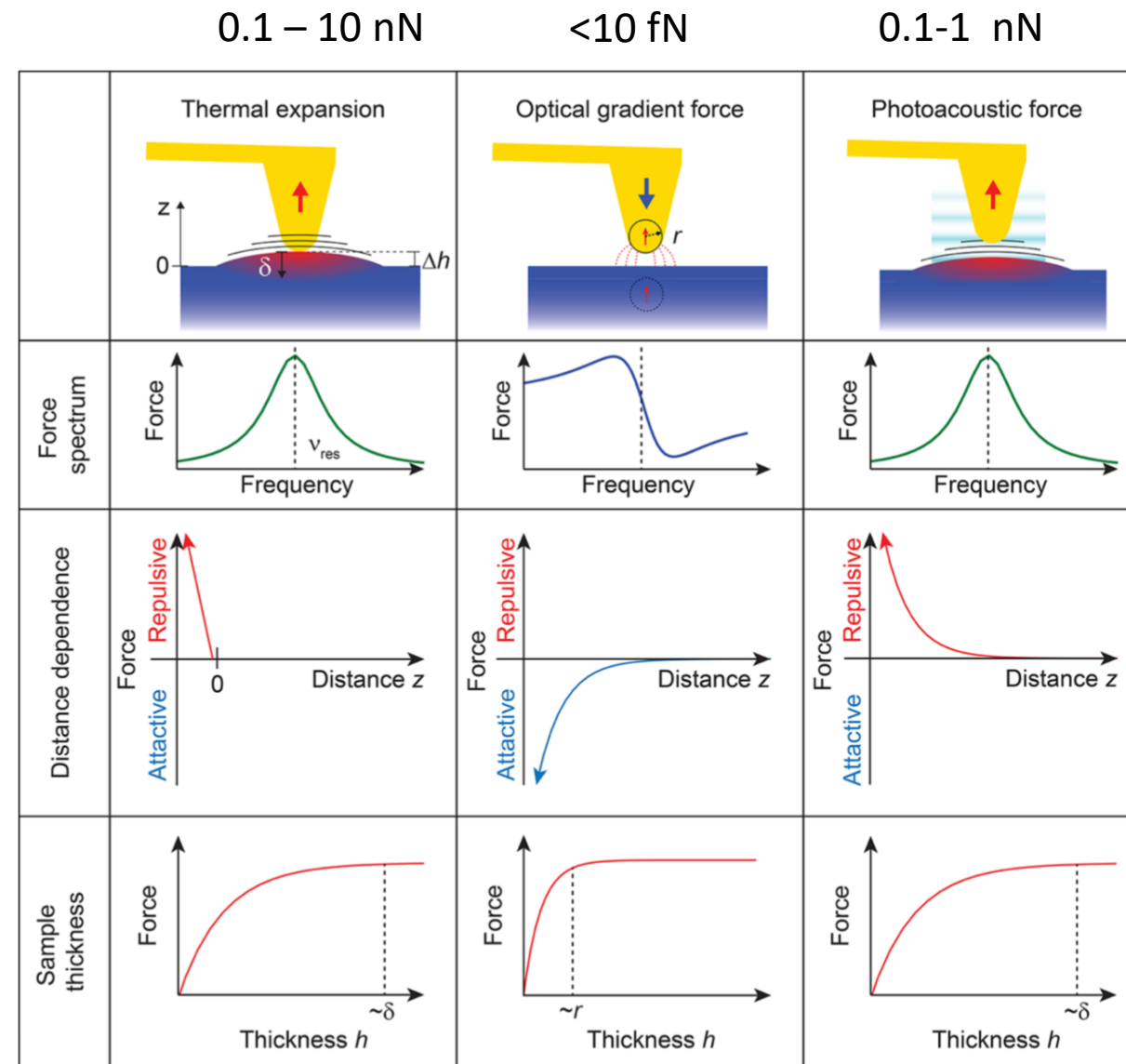
J. Jahng et al. Acc. Chem. Res. , 48, 2671–2679, 2015



$$F \propto \frac{1}{z^4} \operatorname{Re}(\alpha_t) \operatorname{Re}(\alpha_s) E_0^2 \propto \operatorname{Re}(n)$$



5. Comparison with competitors

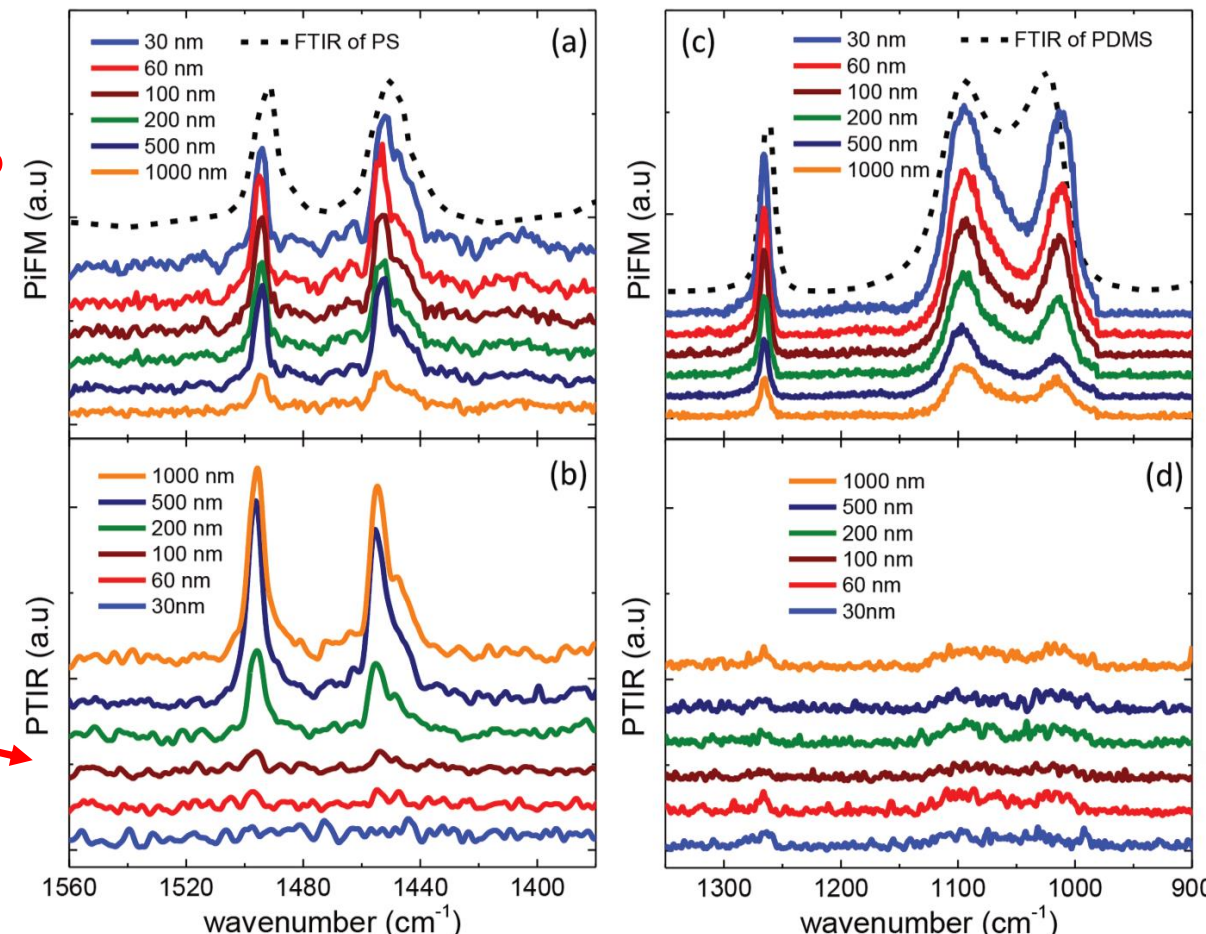


5. Comparison with competitors

- PiFm (Photo-Induced Force microscope)

When conflict of interest (business) meets science

PiFm =Absorbance !?



What a joke ?

CONCLUSION and PERSPECTIVES

- AFM-IR is the only technique that allows a direct measurement of the imaginary part of the refractive index. IR spectrum are comparable to FTIR for amorphous materials.
- Lot of imaging modes : contact resonance, tapping, peakforce, surface sensitive, ForceVolume that allow us to choose the best investigating mode for specific sample and to suit in an optimum way.
- The advantage of AFM versatility open the door to numerous applications in a wide range of scientific domains
- Technique is still evolving : liquid, tomography, controlled environment
- AFMIR community increases each year that stimulate discussion and exchange between scientists



musiics.icp@universite-paris-saclay.fr



Thanks to

AFM-IR lab:

A. Deniset-Besseau



Ariane Deniset-Besseau



Dominique Bazin



Jérémie Mathurin

A. Dazzi

J. Mathurin

D. Bazin

M. Petay

L. Bejach (PhD)



Margaux Petay



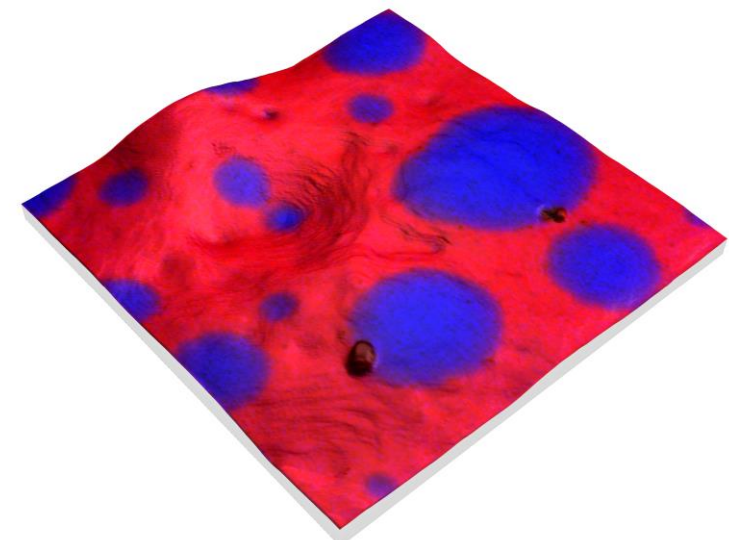
Laure Bejach



Antoine Vite



dépasser les frontières



1. Conventional IR spectroscopy and imaging

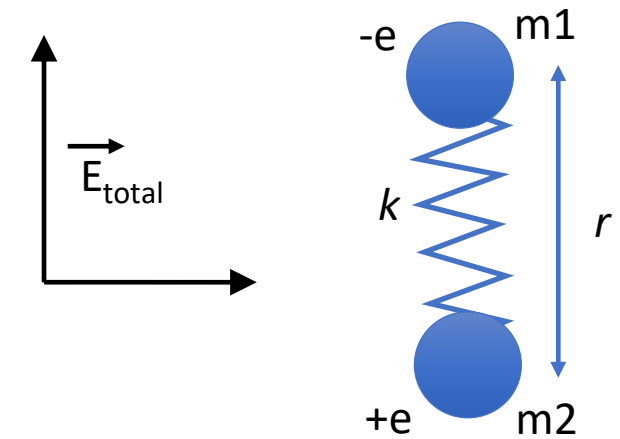
Polarisation is defined by:

$$P = Np = N\alpha_p E_{total} = \epsilon_0 \chi E$$

where N number of bonds, α_p polarisability,
 ϵ_0 vacuum permittivity and χ dielectric susceptibility

Refractive index can be expressed by:

$$n^2 = 1 + \chi = 1 + \chi_0 + \frac{3N\alpha_p}{3\epsilon_0 - N\alpha_p}$$



$$\omega_0 = \sqrt{k/m}$$

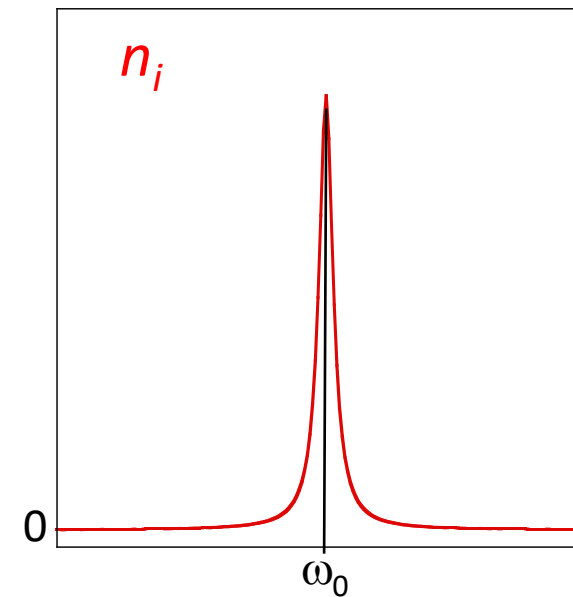
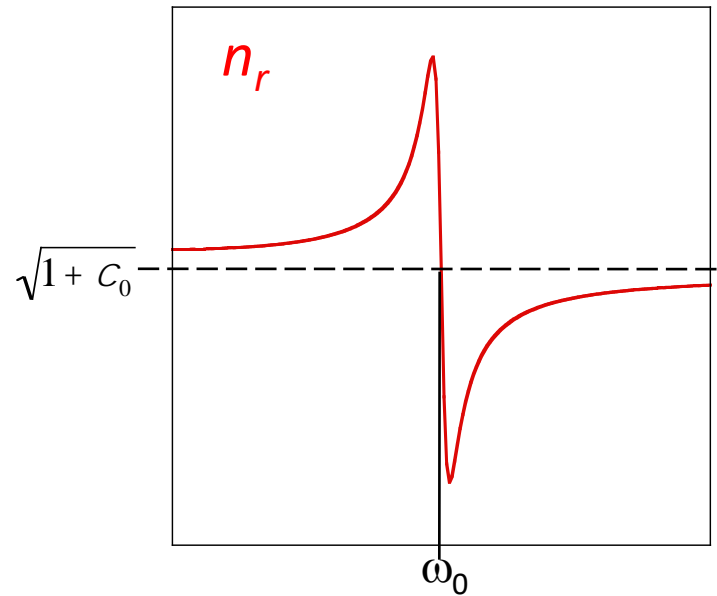
$$\frac{1}{m} = \frac{1}{m_1} + \frac{1}{m_2}$$

1. Conventional IR spectroscopy and imaging

Refractive index expression can be written :

$$n^2 = n_r^2 - n_i^2 + i2n_r n_i = 1 + C_0 + (N/e_0) \frac{(e^*)^2 / m (w_0^2 - w^2)}{(w_0^2 - w^2)^2 + (wb/m)^2} + i(N/e_0) \frac{bw(e^*/m)^2}{(w_0^2 - w^2)^2 + (wb/m)^2}$$

Considering organic material, then imaginary part of the index is always smaller than real part ($n_i \ll n_r$).
This approximation allow to have a simple expression of n_i represented by a Lorentzian function



$$n_i = \frac{(N/e_0)}{2\sqrt{1 + C_0}} \frac{bw(e^*/m)^2}{(w_0^2 - w^2)^2 + (wb/m)^2}$$

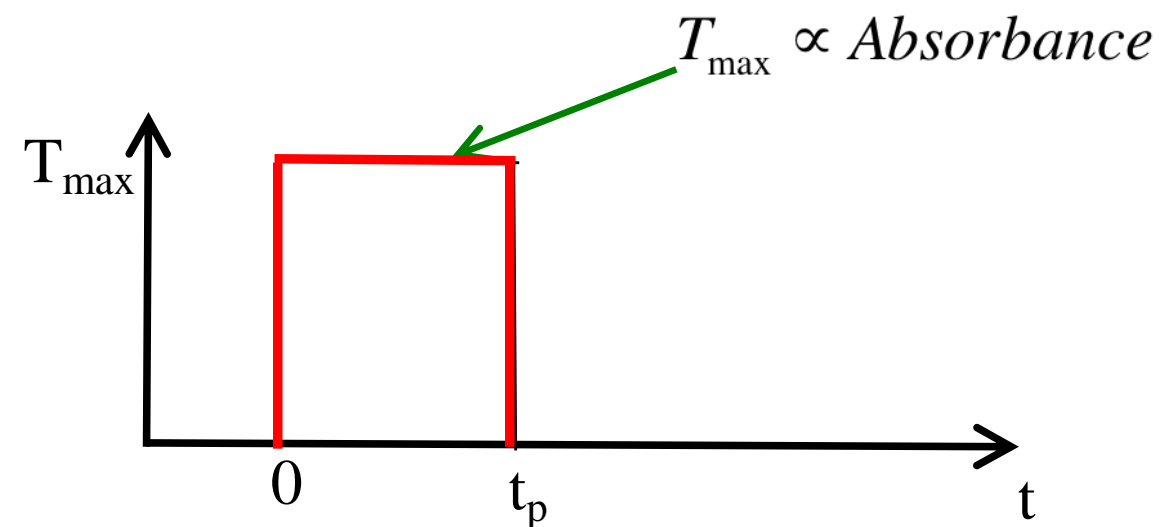
2. AFM-IR theory and concept

Temperature evolution of the sphere $(a \ll L)$

$$T(t) = T_{max} = \frac{P_{abs}}{4\pi a K_{sph}} \quad \text{when } 0 \leq t \leq t_p$$

when $t_p \gg |_{\text{relax}}$

$$T(t) = 0 \quad \text{when } t_p < t$$



2. AFM-IR theory and concept

Relaxation time τ_{relax} exemple for polymer sphere (PMMA):

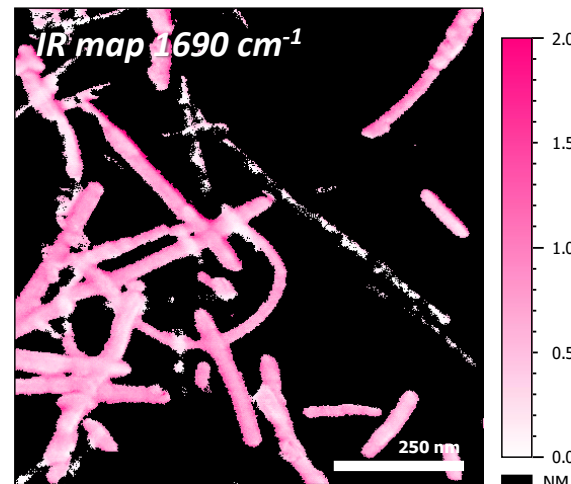
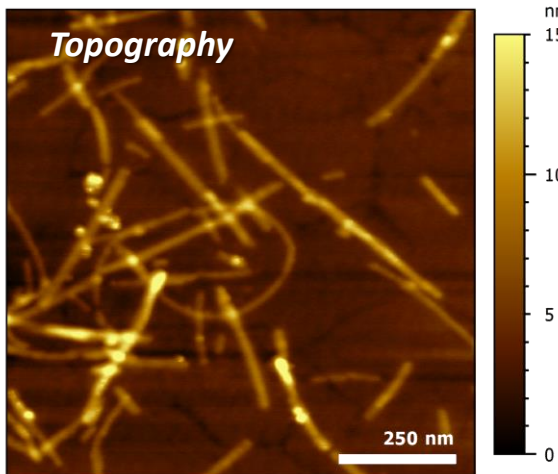
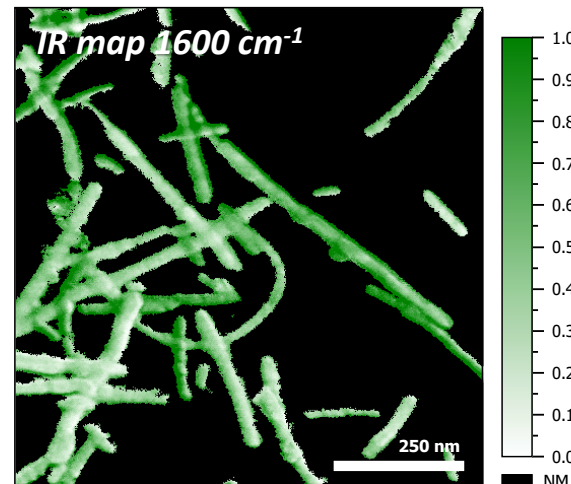
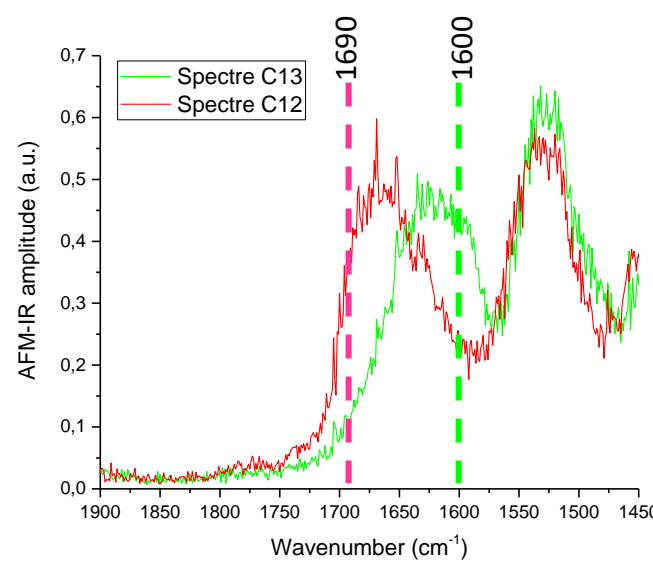
K_{ext}	a	10 μm	1 μm	100 nm	10 nm
air 0.025 $\text{Wm}^{-1}\text{K}^{-1}$		2.3 ms	22.7 μs	227 ns	2.3 ns
water 0.58 $\text{Wm}^{-1}\text{K}^{-1}$		98 μs	980 ns	9.8 ns	98 ps
silica 1.38 $\text{Wm}^{-1}\text{K}^{-1}$		41 μs	411 ns	4 ns	41 ps
gold 317 $\text{Wm}^{-1}\text{K}^{-1}$		0.18 μs	1.8 ns	18 ps	0.18 ps

$$\tau_{\text{relax}} = \frac{\rho_{\text{sph}} C_{\text{sph}}}{3 K_{\text{ext}}} a^2$$

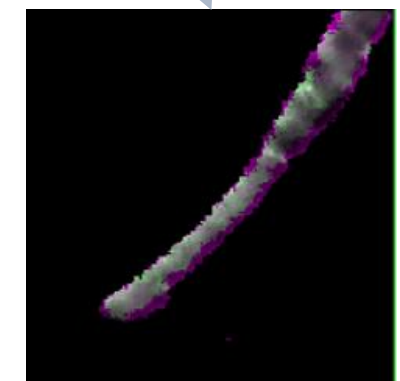
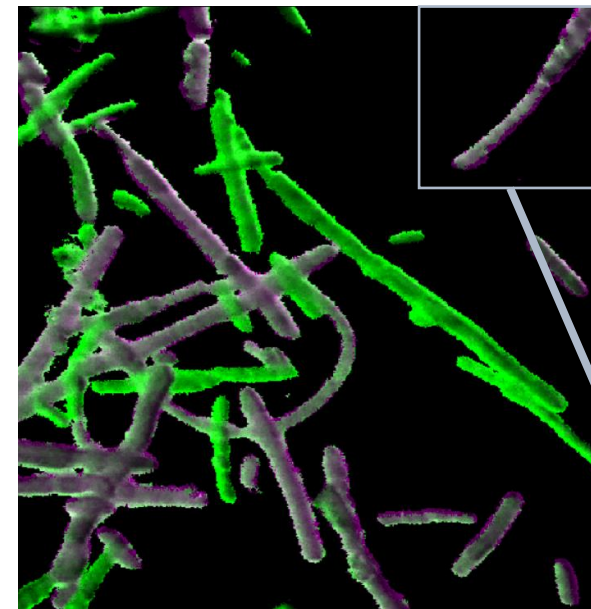
$$\rho = 1200 \text{ kg m}^{-3}, C = 1420 \text{ J kg}^{-1} \text{ K}^{-1}$$

3. Applications examples

Prions amyloid fibers analysis



Composite G ($C_{13} >> C_{12}$), M ($C_{12} >> C_{13}$)



Collab. H.Rezaei INRA Jouy-en-Josas

Silica beads in polystyren film

